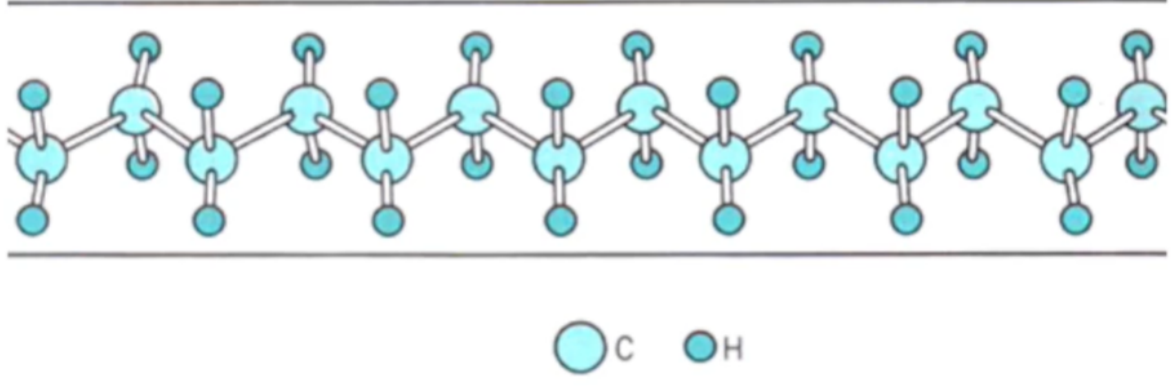


# Polymers

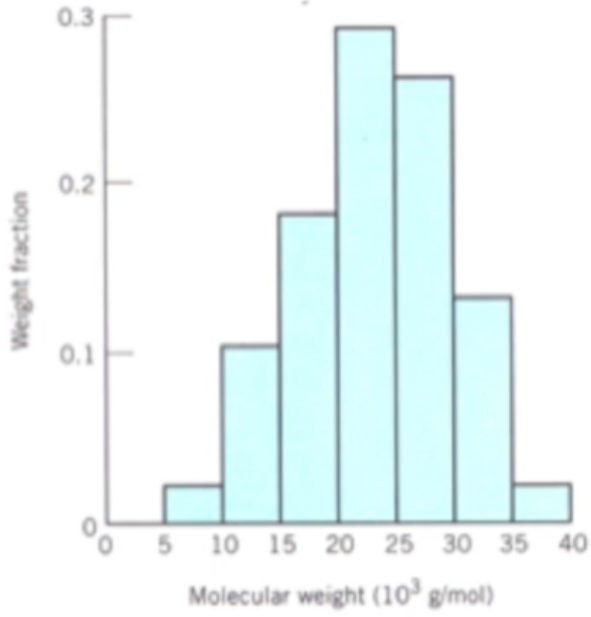
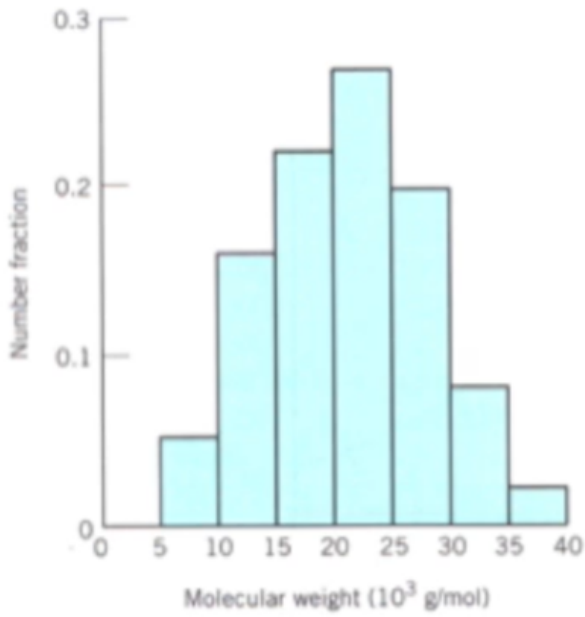
*There is and never will be such a thing as a macromolecule*

1915

*The development of polymerization is, perhaps, the biggest thing chemistry has done.*



C H



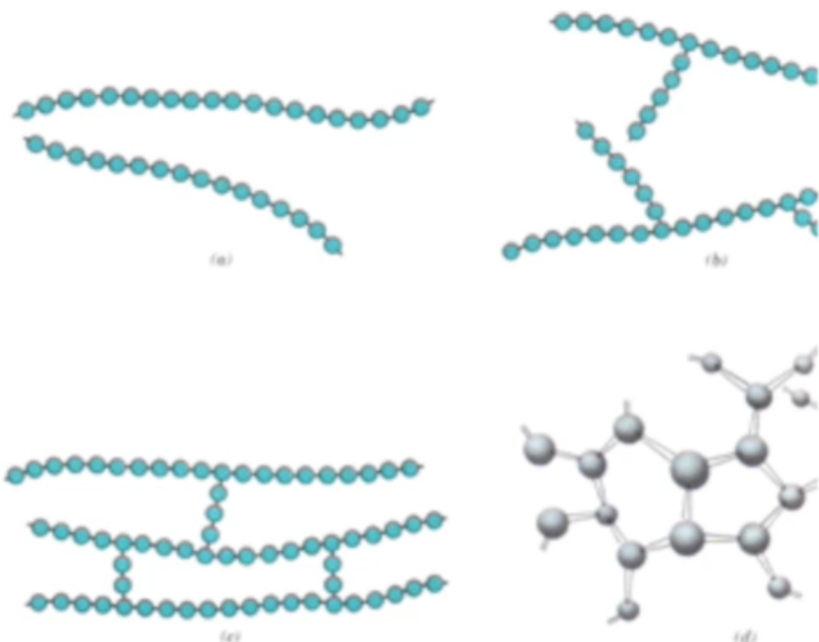
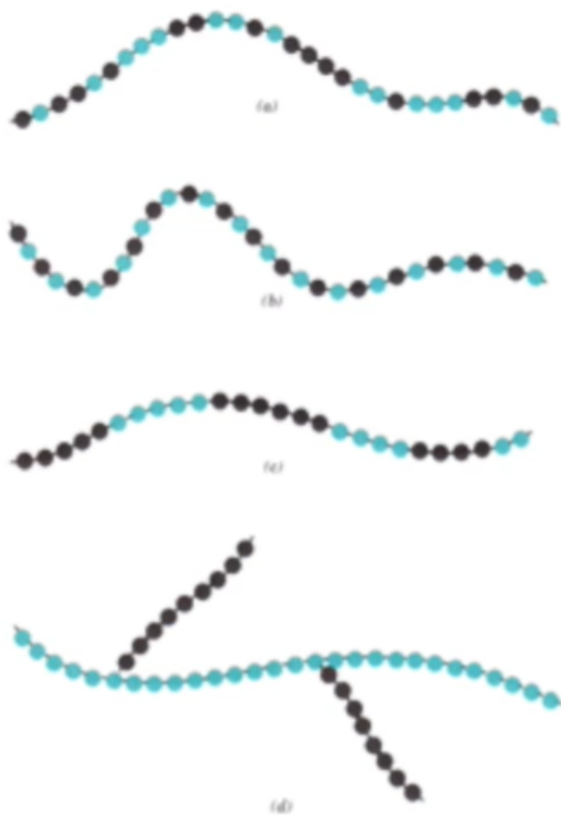
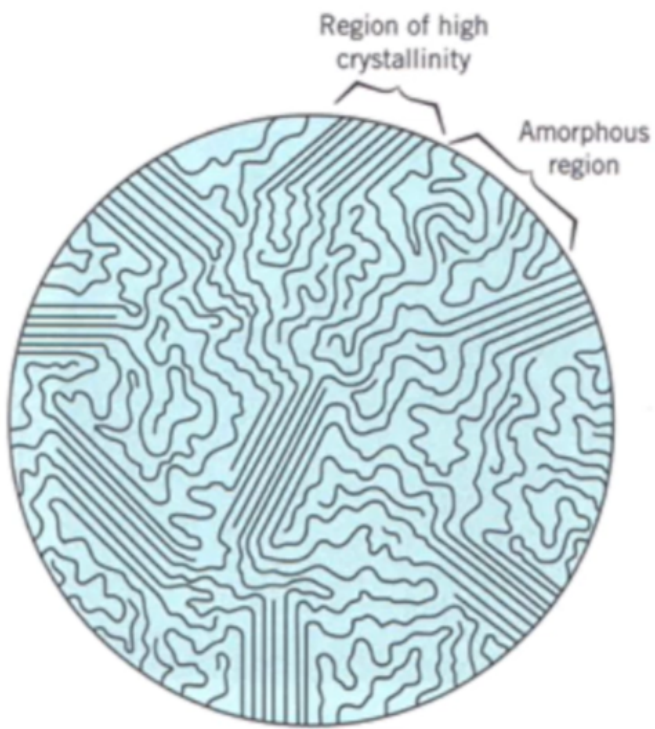


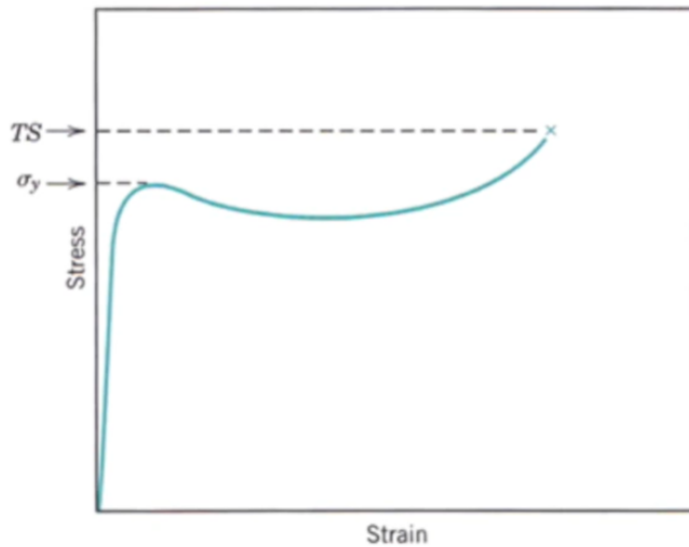
FIGURE 15.7 Schematic representations of (a) linear, (b) branched, (c) crosslinked, and (d) network (three-dimensional) molecular structures.

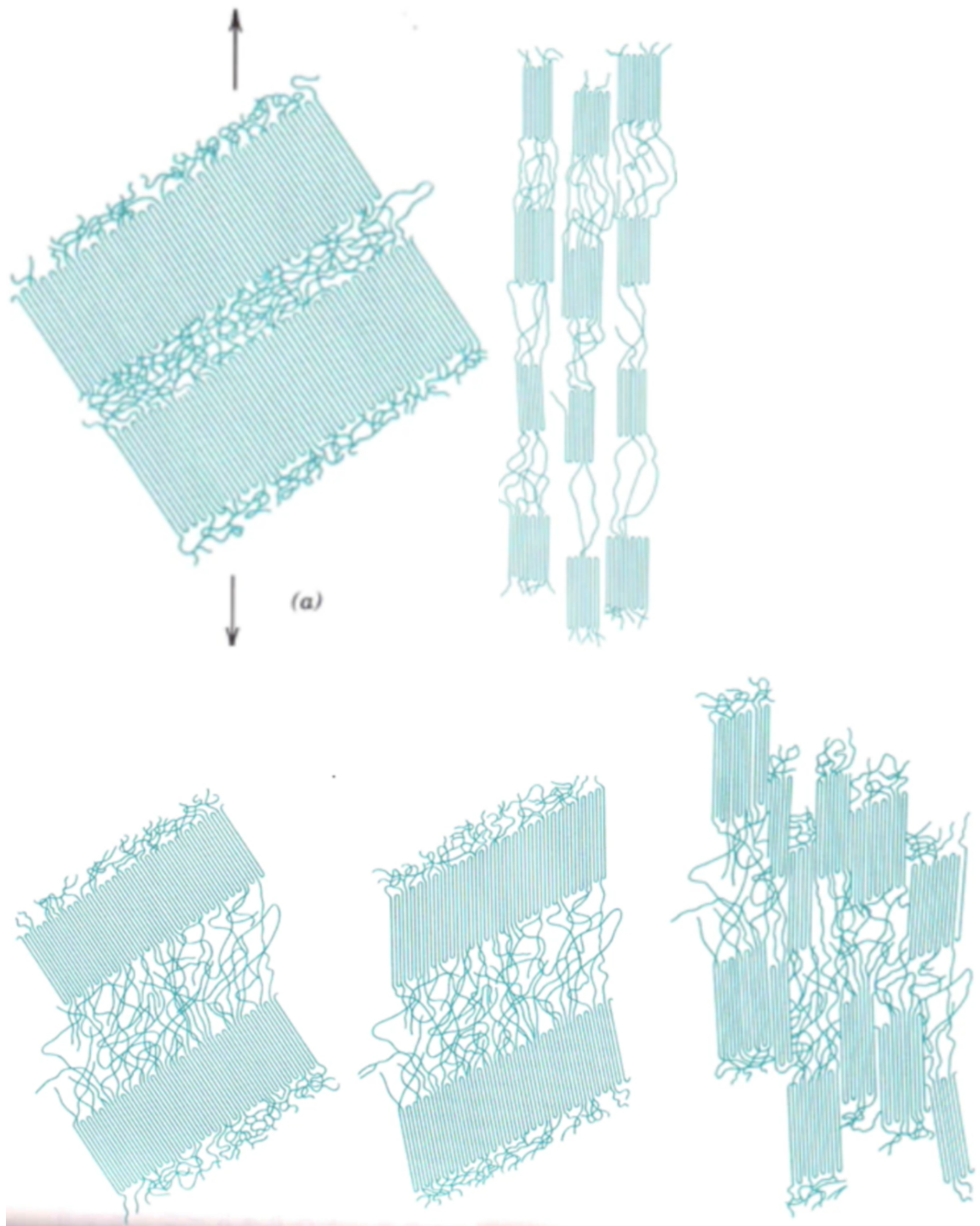
FIGURE 15.8  
Schematic representations of (a)  
random, (b) alternating,  
(c) block, and (d) graft  
copolymers. The two  
different mer types are  
designated by black and  
colored circles.

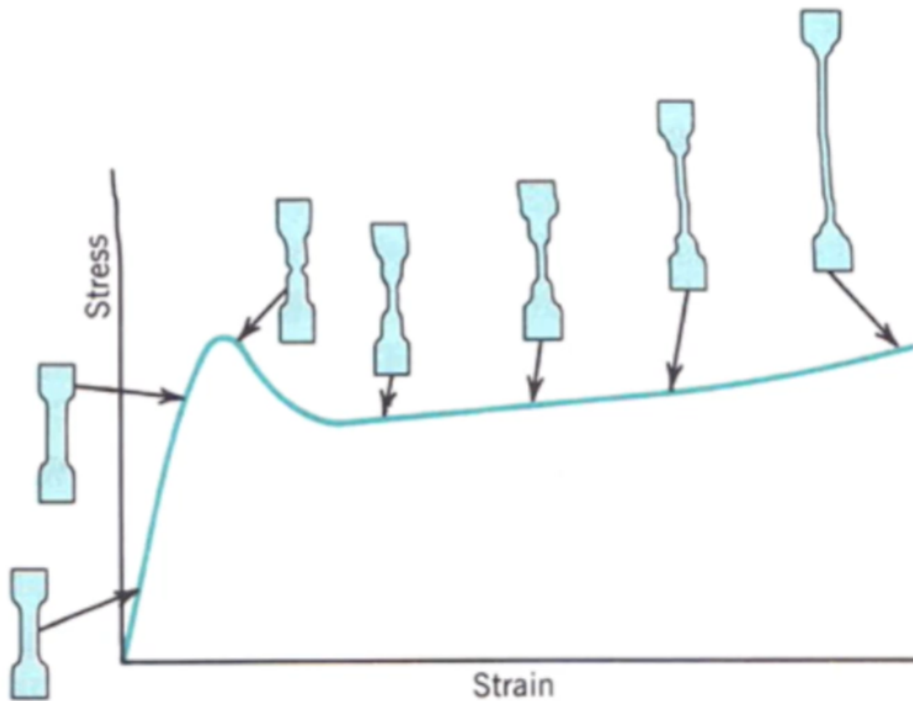




## Stress-strain curve







## Temperature effect

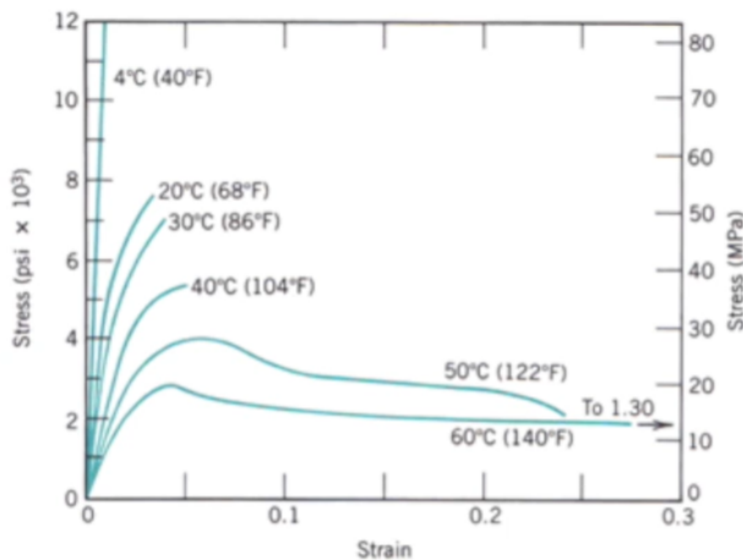
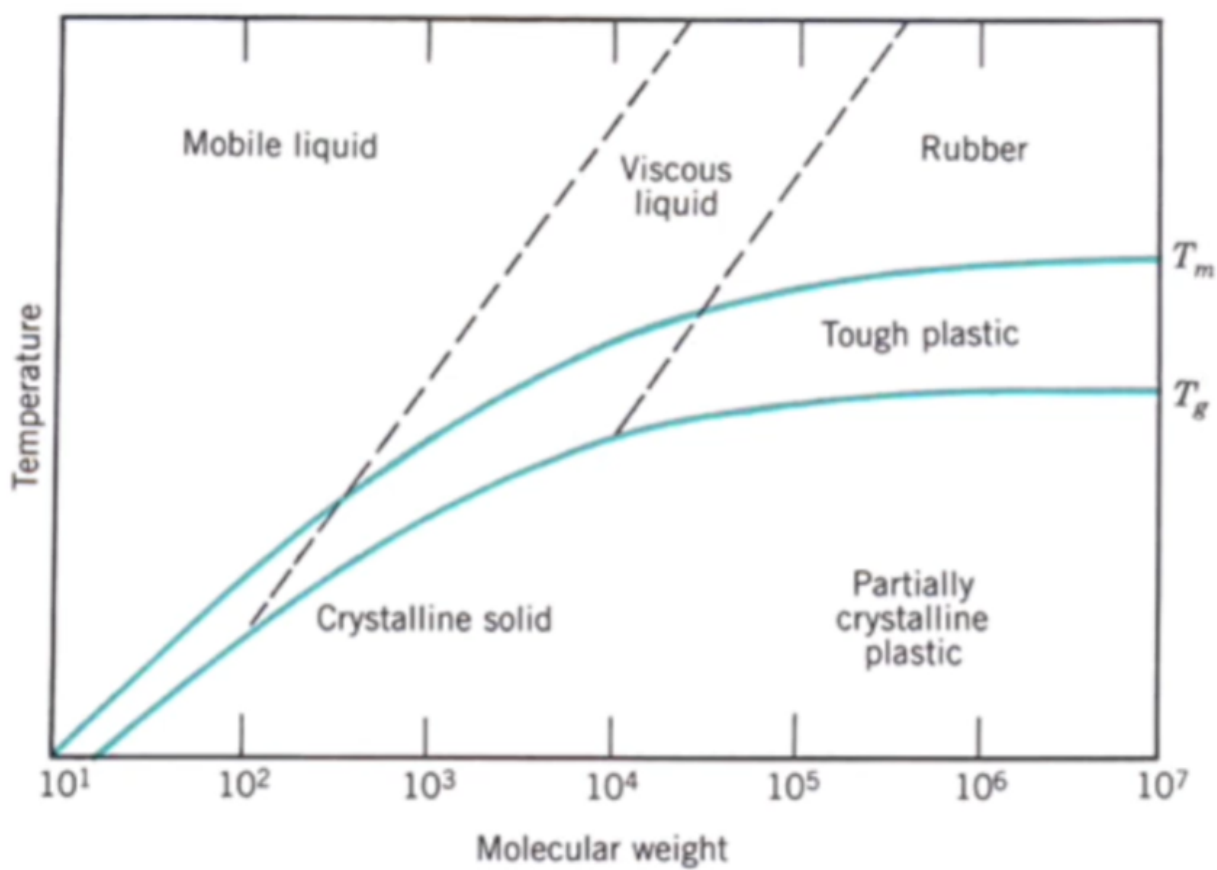
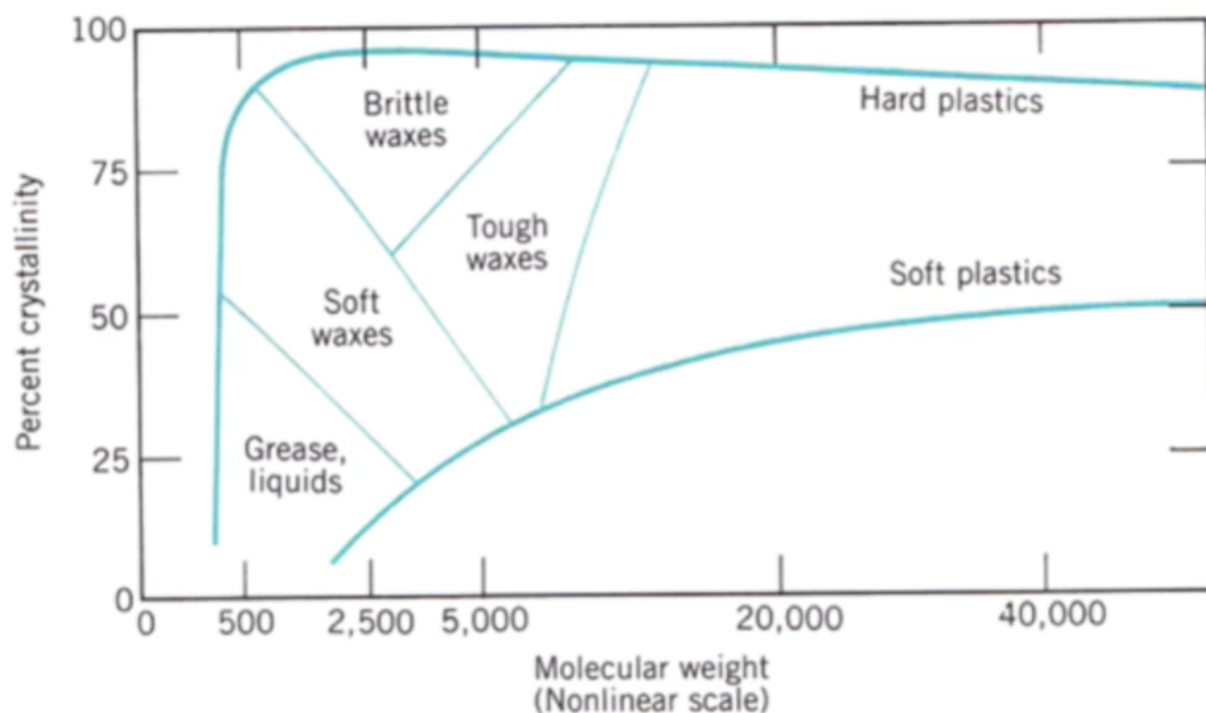


**FIGURE 16.3** The influence of temperature on the stress-strain characteristics of polymethyl methacrylate. (From T. S. Carswell and H. K. Nason, "Effect of



# Viscoelastic / viscoplastic behaviour

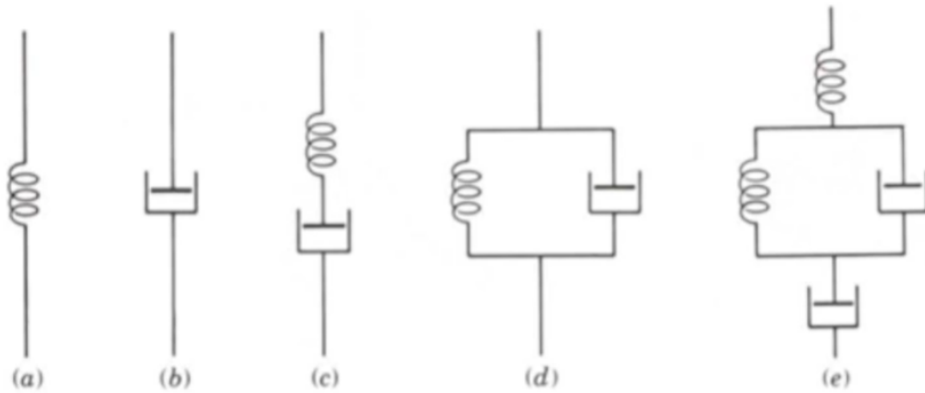
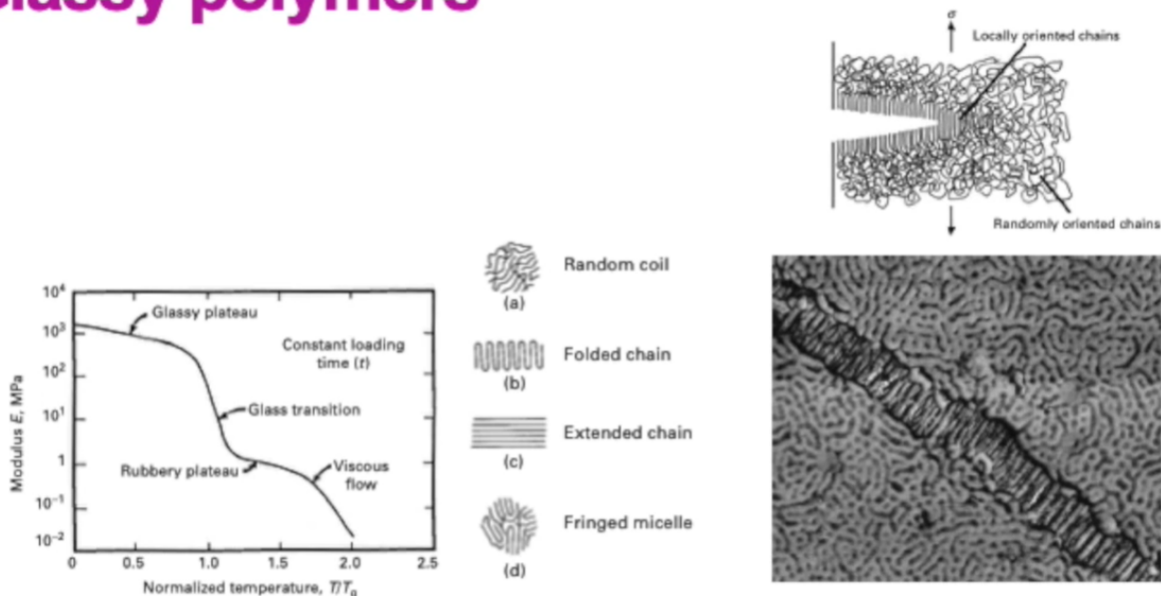
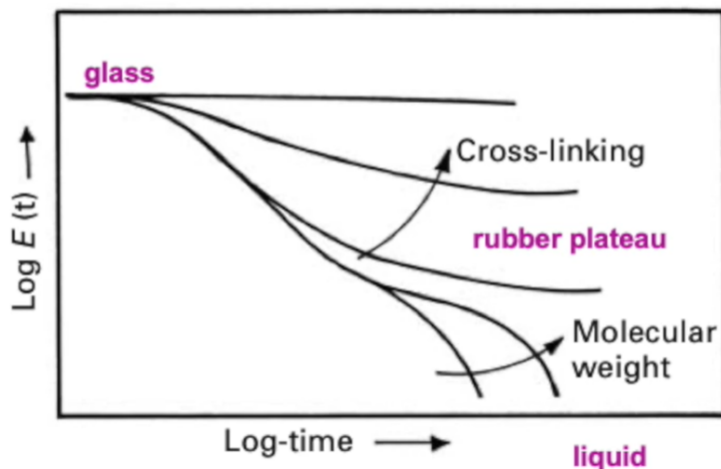


FIGURE 6.20 Mechanical analogs reflecting deformation processes in polymeric solids: (a) elastic; (b) pure viscous; (c) Maxwell model for viscoelastic flow; (d) Voigt model for viscoelastic flow; (e) four-element viscoelastic model.

## Glassy polymers

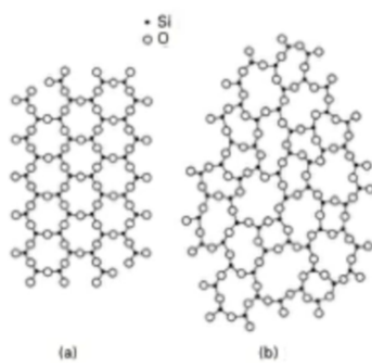


## Cross-linking

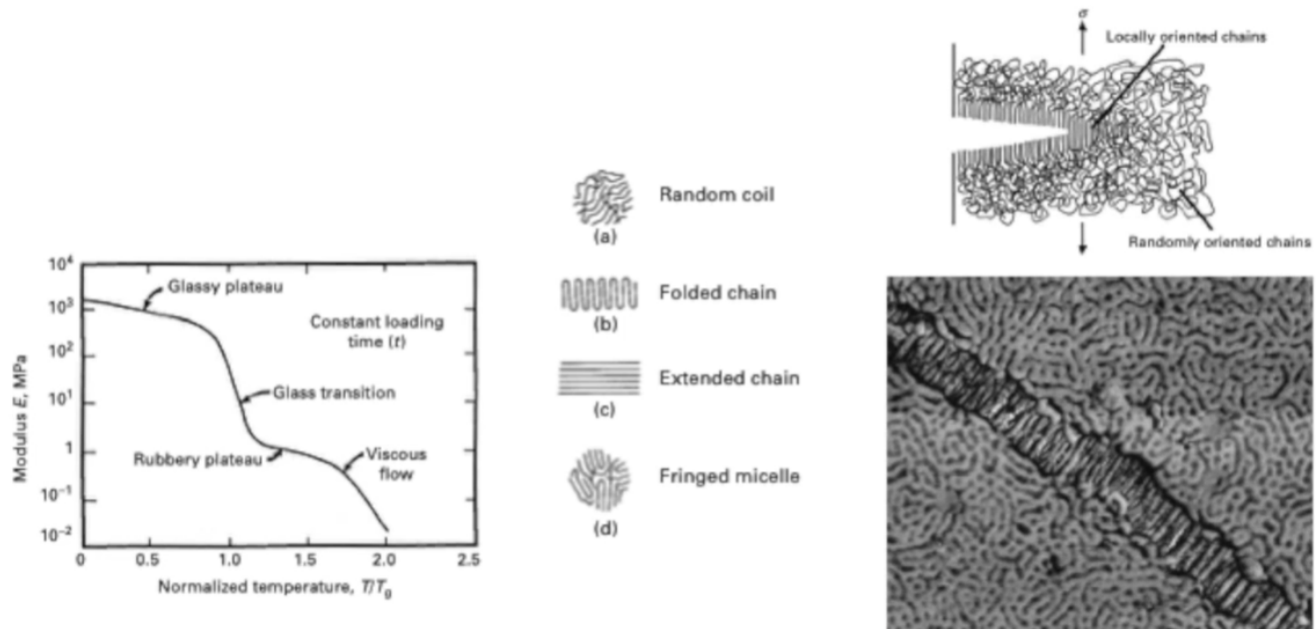


# Deformation in glasses

## Network glasses

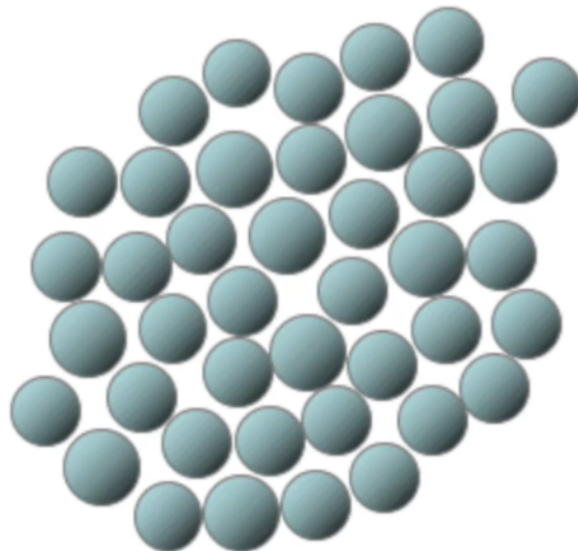


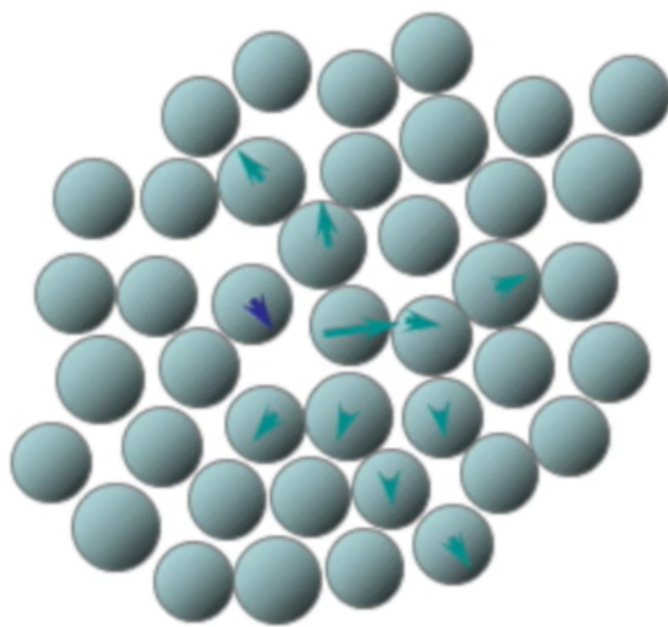
# Glassy Polymers



## Reorganization

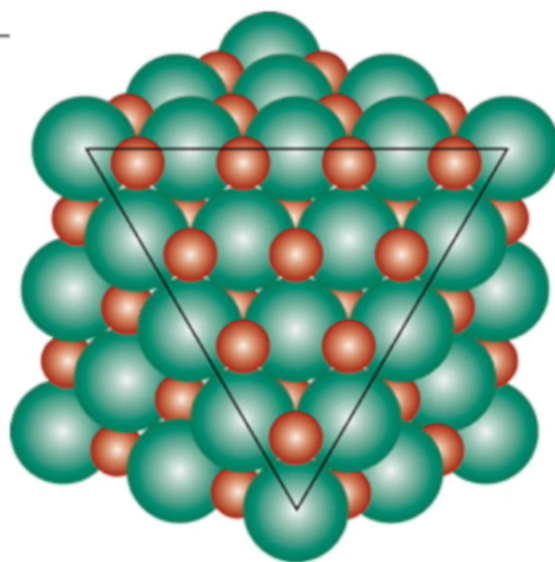
Least-energy deformation activates number of atoms



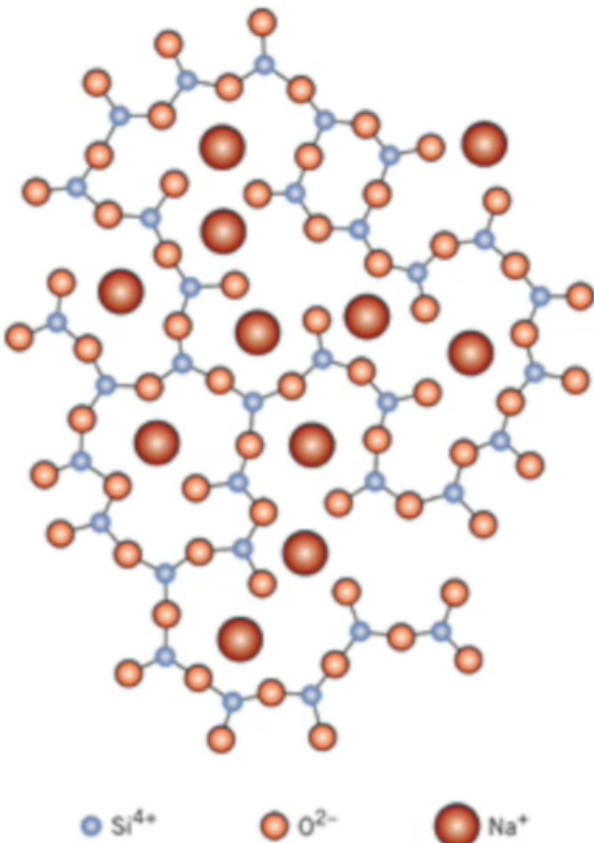


# Ceramics

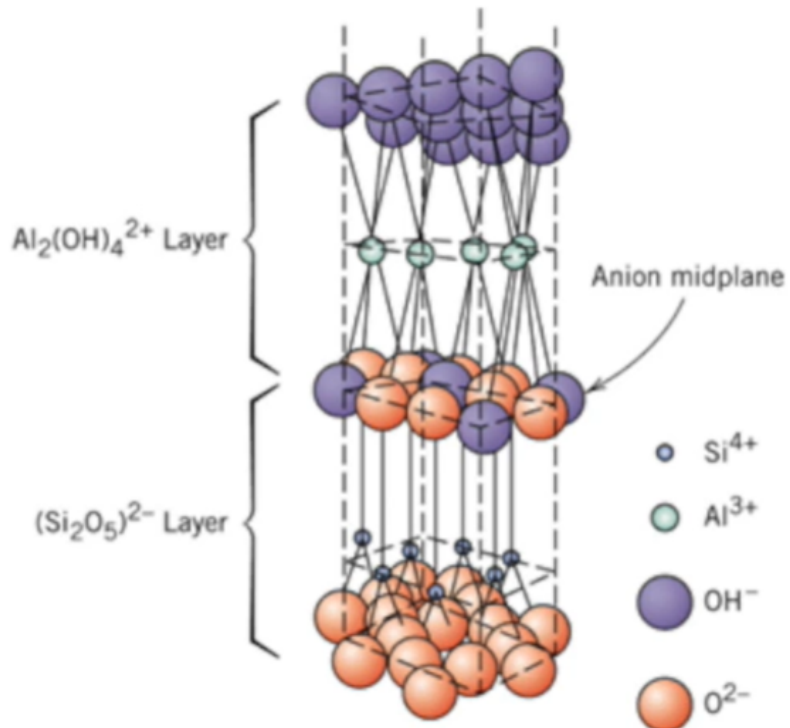
Crystalline...



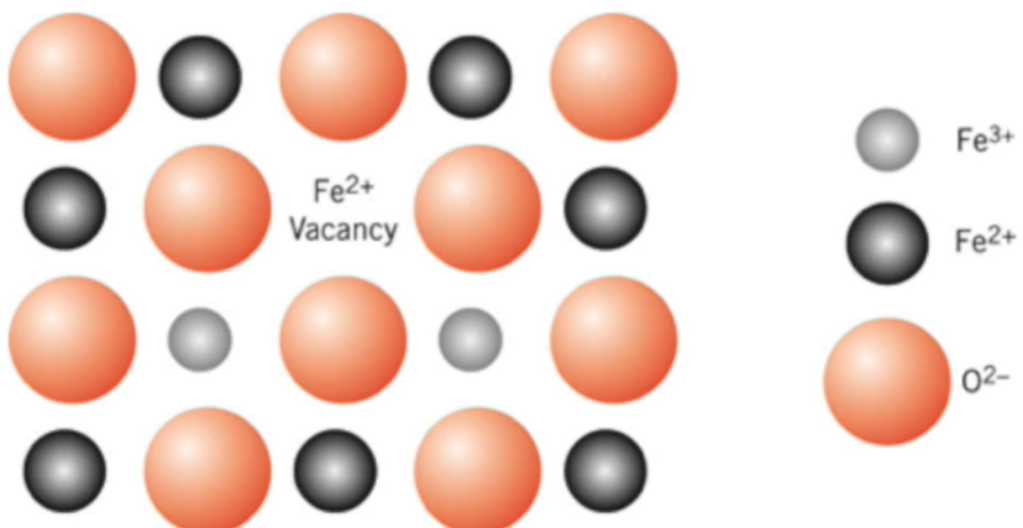
# ...amorphous



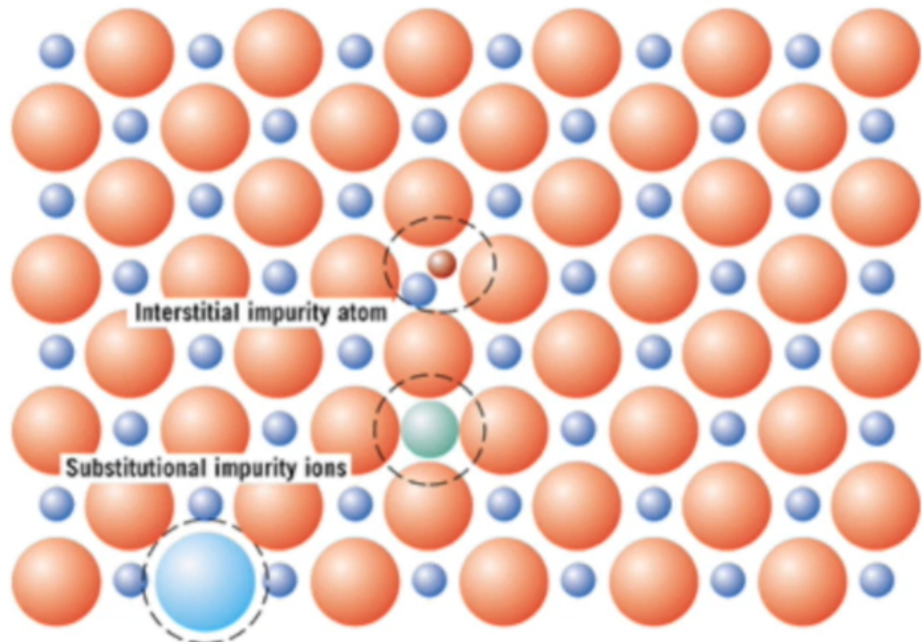
# Layered



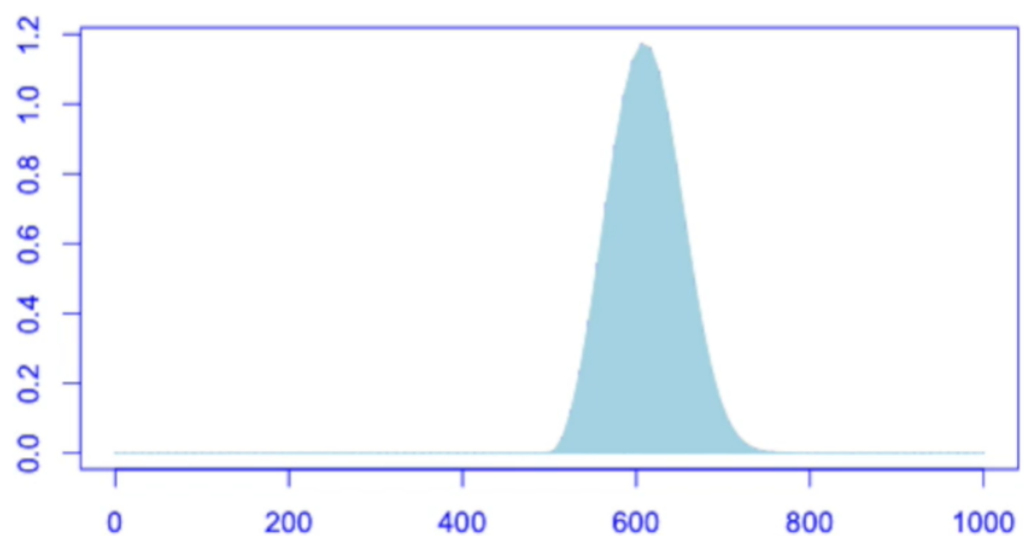
# Stoichiometry



# Impurities and lattice defects



**Strength is variable**



# Intermetallics

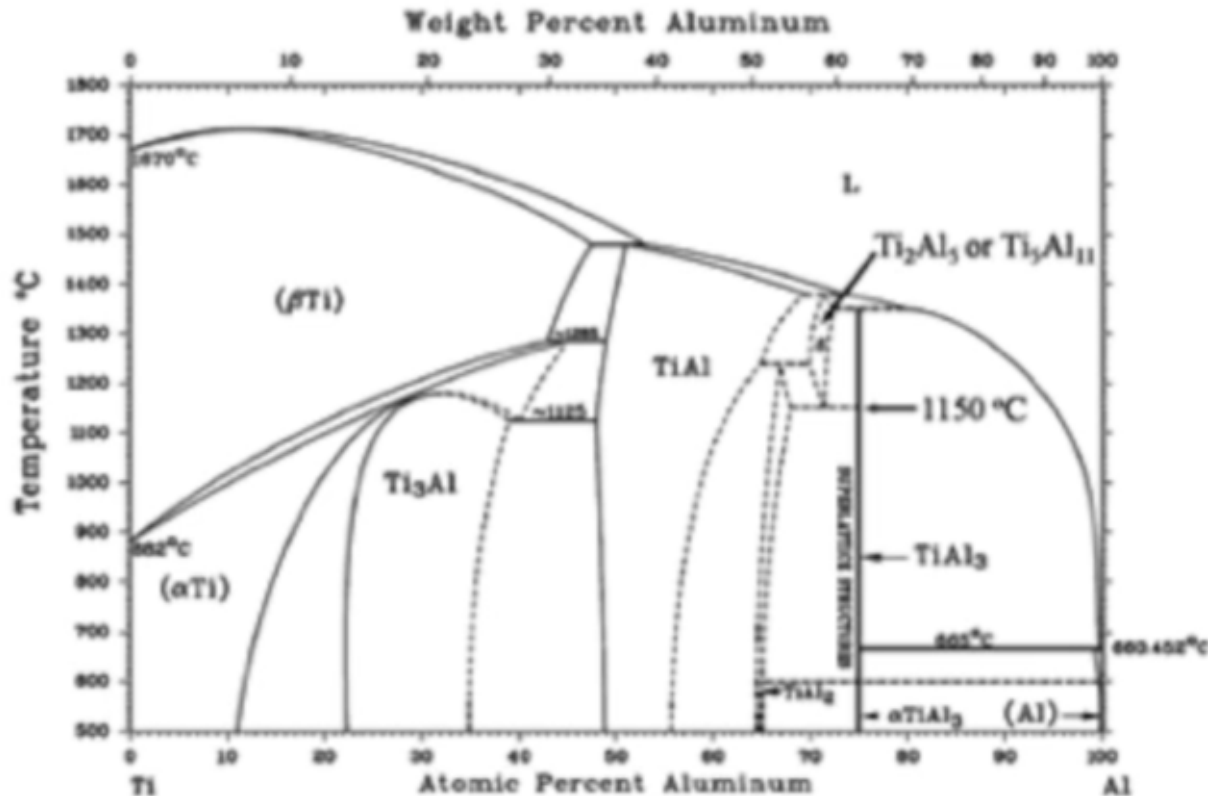
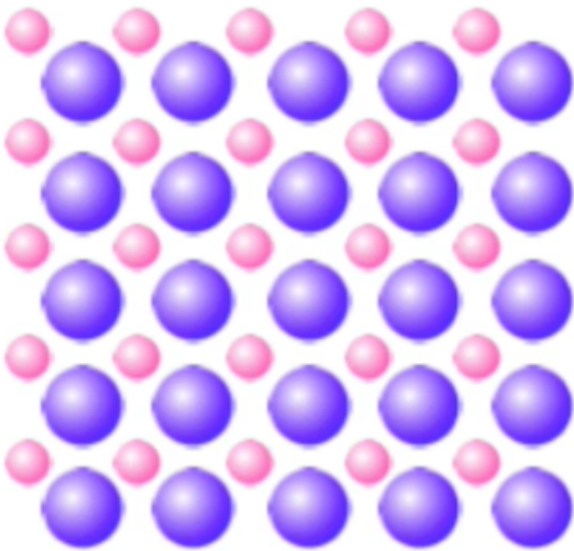


Fig. 3. Phase diagram in Ti-Al system.

# **Superlattice**



## **Metallic and ceramic properties**

**Metallic bond**

**Directed**

**Difficult plastic deformation**

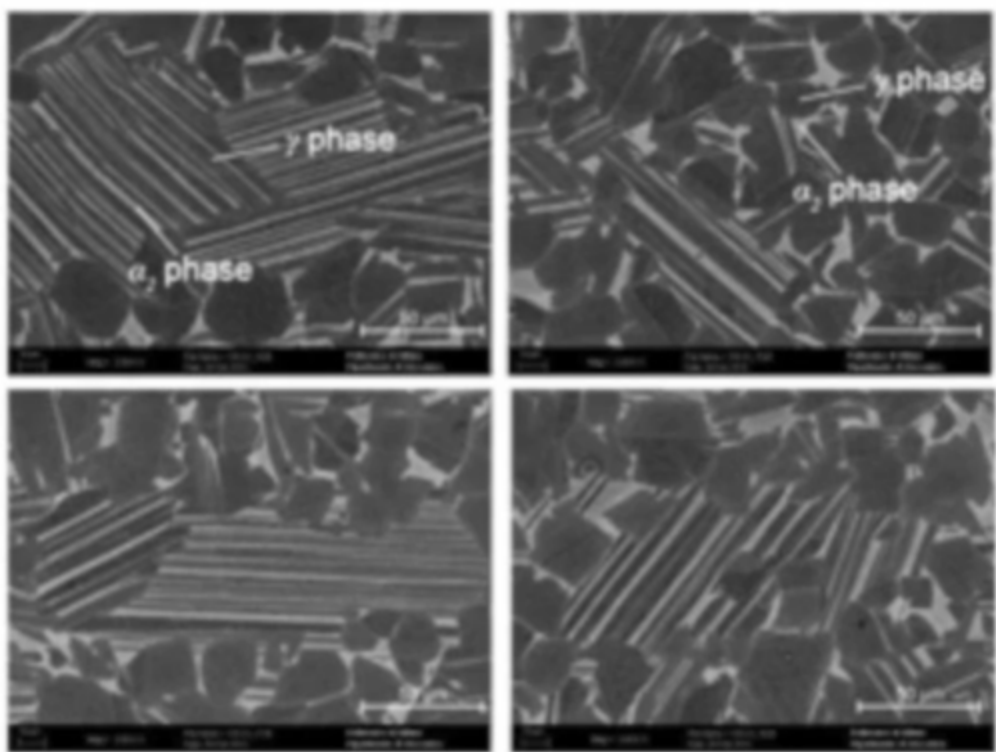


Figure 1. MICROGRAPHS CAPTURED THROUGH SCANNING ELECTRON MICROSCOPY SHOWING THE TYPICAL CONFIGURATION OF THE MICROSTRUCTURE FOR THE  $\gamma$ -TIAL ALLOY USED IN THIS WORK.

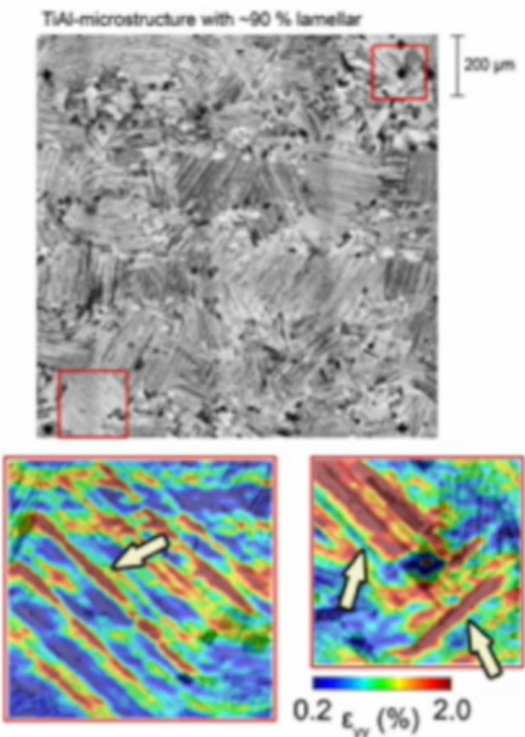


Figure 7b. HIGH RESOLUTION DIC STRAIN OBTAINED EX\_SITU MEASUREMENTS OBTAINED IN COMPRESSION AT A NOMINAL STRESS OF  $\sigma=450$  MPa AFTER 100 CYCLES FOR A FULLY LAMELLAR MICROSTRUCTURE.

## Coatings

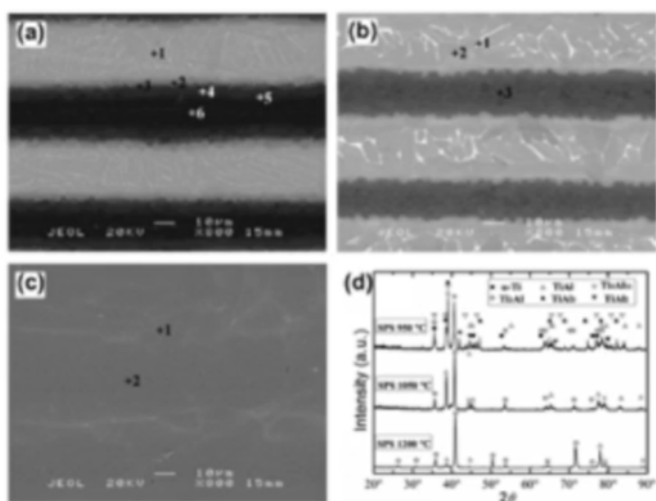
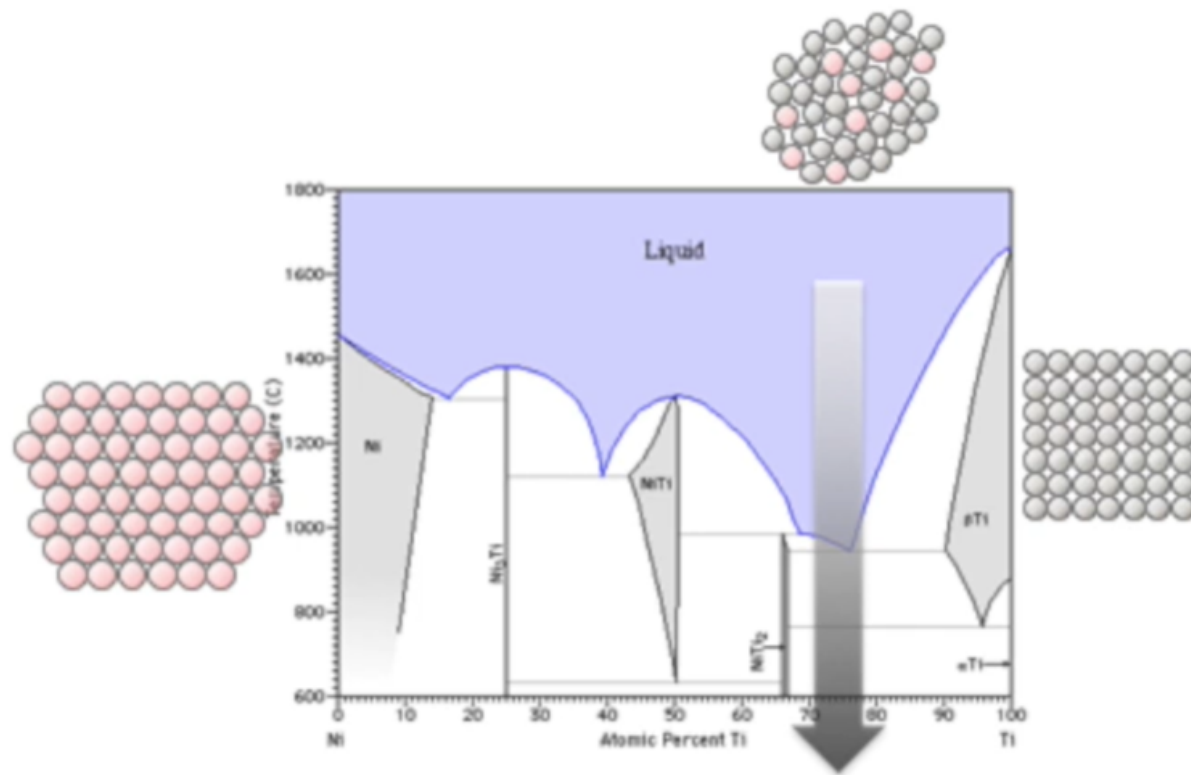


Fig. 4. The TiAl multilayered sample with spark plasma sintering under 50 MPa for 10 min with different temperature: (a) back scattered electron image for sintering at 950 °C; (b) back scattered electron image for sintering at 1050 °C; (c) back scattered electron image for sintering at 1200 °C; (d) X-ray diffraction patterns for different sintering temperatures.

# Metallic glasses



## Matrix + reinforcement

Reinforcement bears the load

- big E
- high strength
- high hardness

Matrix bears the shear stress

Matrix gives ductility

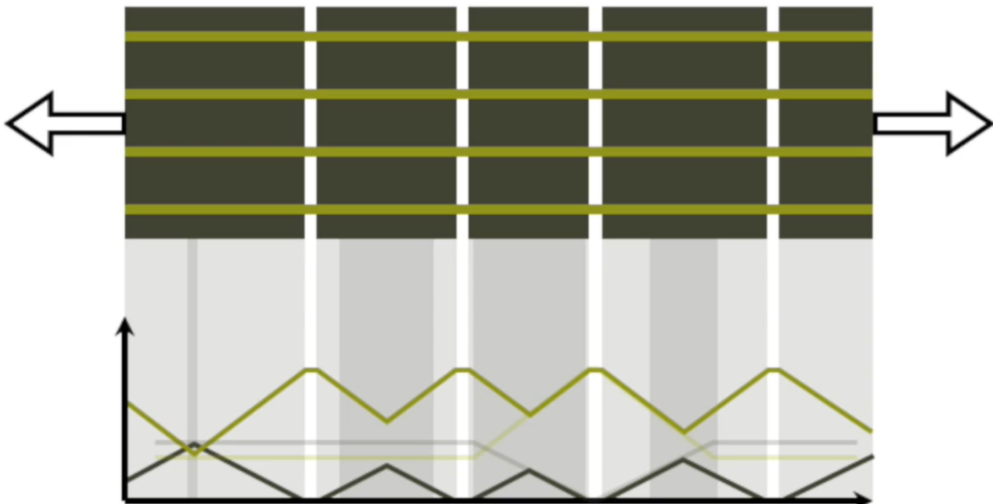
# Failure

reinforcement failure ≠ matrix failure ≠ bond failure

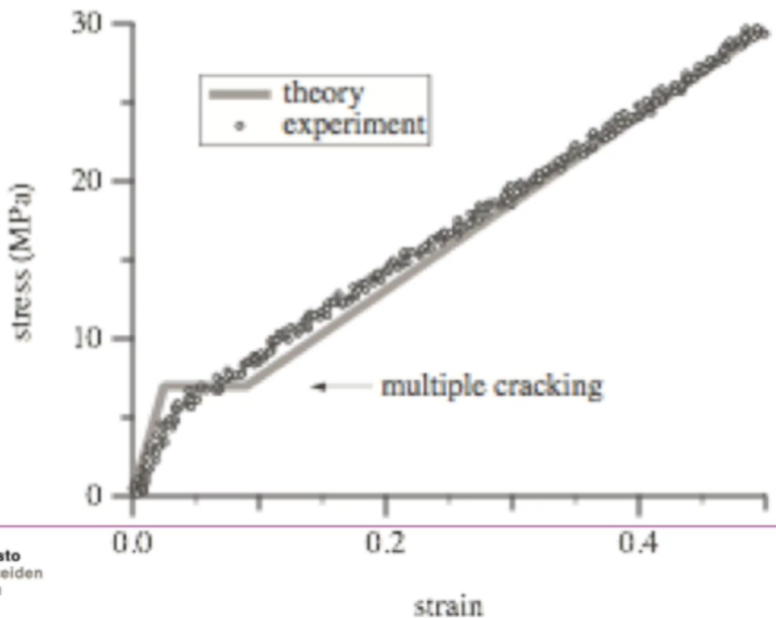
## Load Redistribution



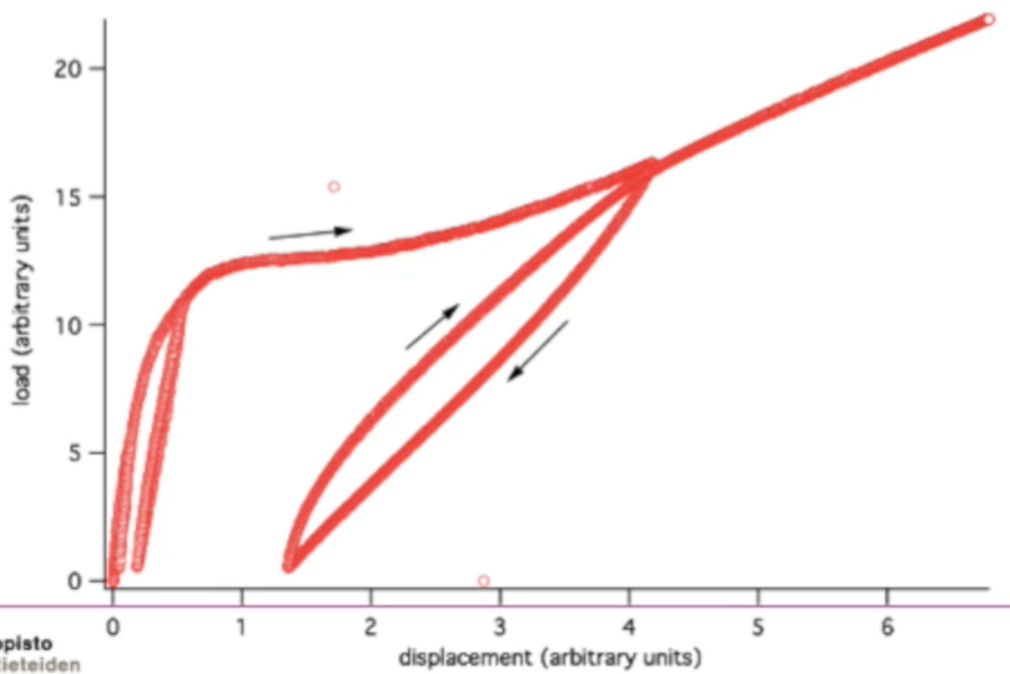
## Load Redistribution



## Stochastic Matrix Cracking



## Stiffness Reduction



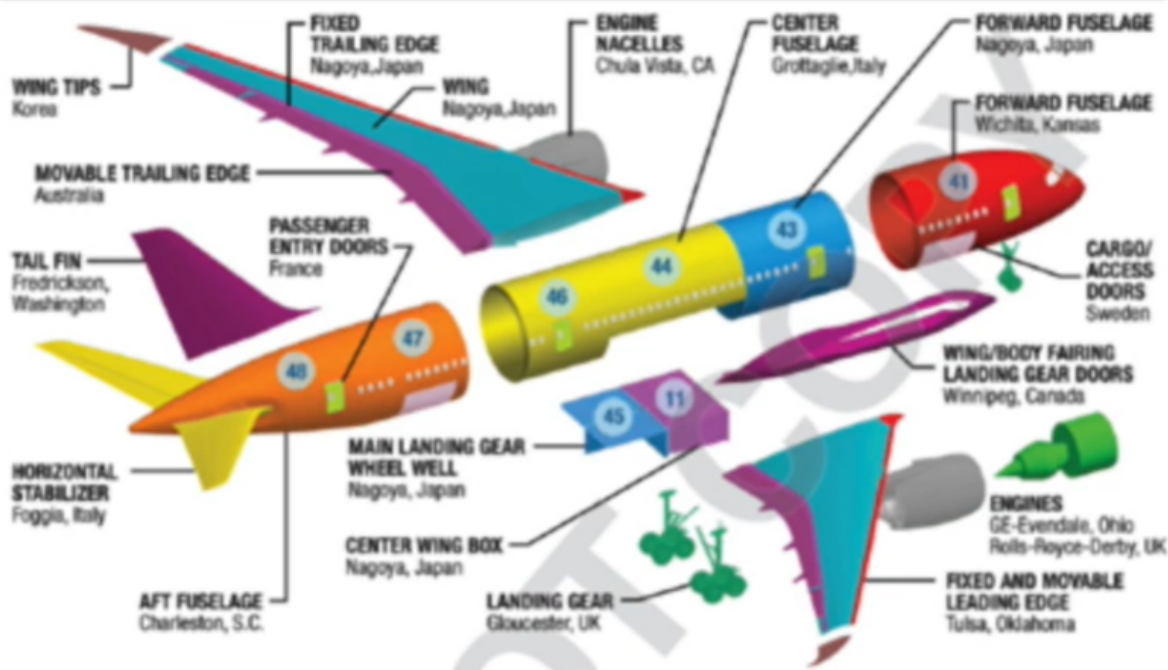
# Polymer matrix composites



Fig. 1. Boeing 787 Dreamliner, showing breakdown of materials used and the MTE designed and manufactured by HdH.

## THE COMPANIES

U.S.	CANADA	AUSTRALIA	JAPAN	KOREA	EUROPE
Boeing	Boeing	Boeing	Kawasaki	KAL-ASD	Messier-Dowty
Spirit	Messier-Dowty		Mitsubishi		Rolls-Royce
Vought			Fuji		Latecoere
GE					Alenia
Goodrich					Saab



# Metallic matrix composites

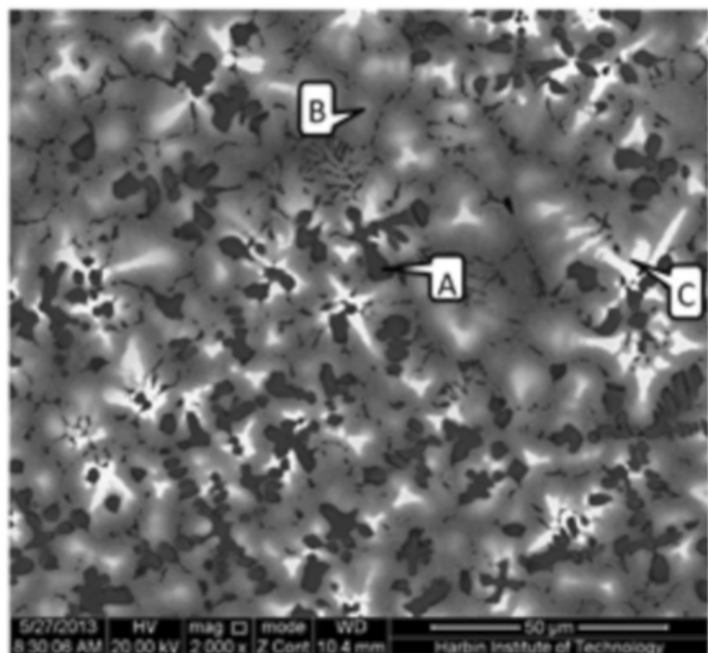


Fig. 10. SEM of MMC layer produced by WPDIL (EDX analysis of A, B, and C shown in Table 2).

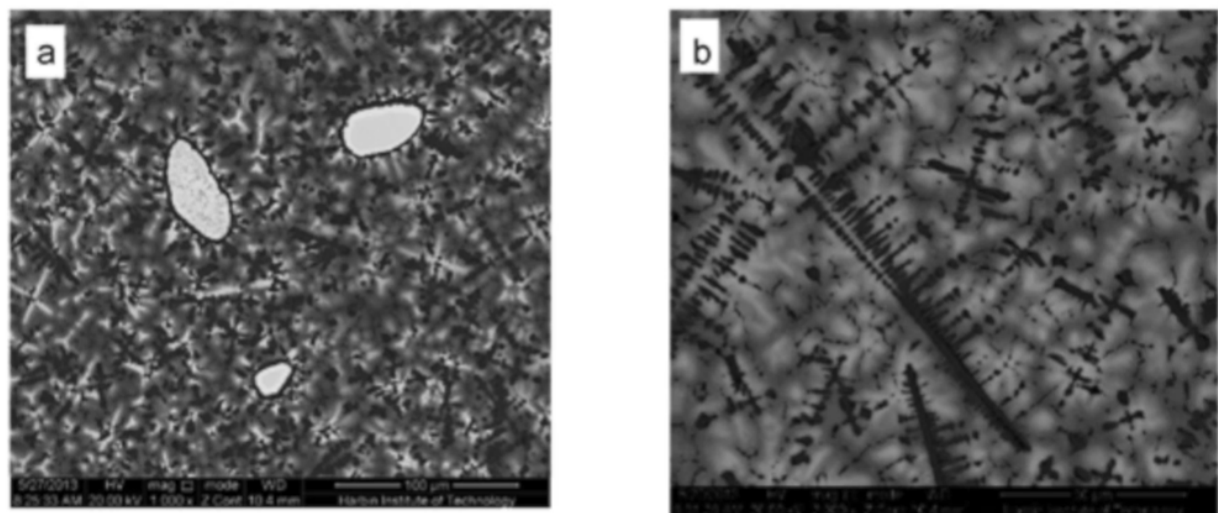
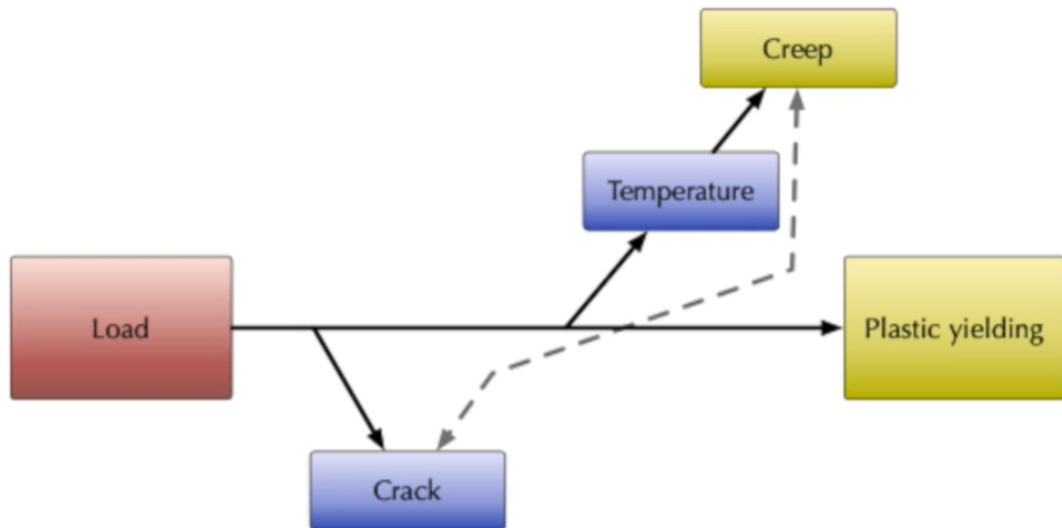


Fig. 12. Morphology of WC particles and TiC at the upper part of MMC layer (a) morphology of WC particle (b) morphology of TiC.

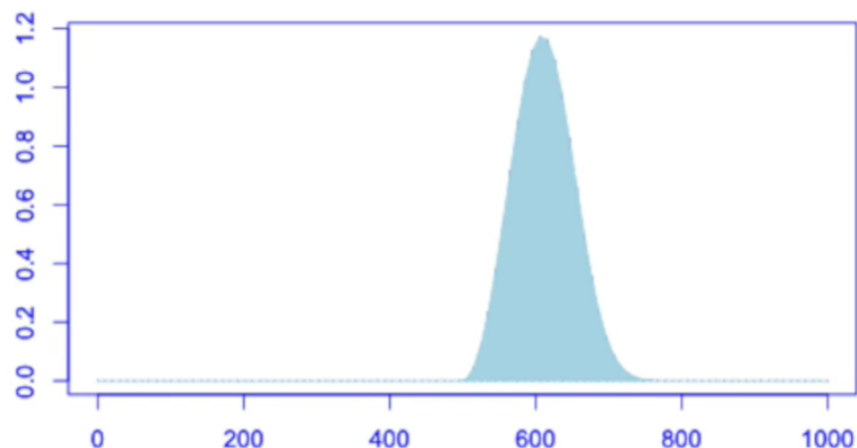
# Fracture mechanics I - the basics

*What are cracks?*

*Where is fracture mechanics used?*



Ceramics: *Why* strength below theoretical?



# Why *brittle* materials break with low stress?

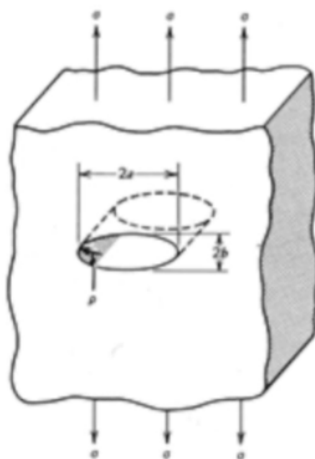




# *Why normally ductile materials show **brittle** **behaviour?***

# Stress concentration

Inglis (1913):

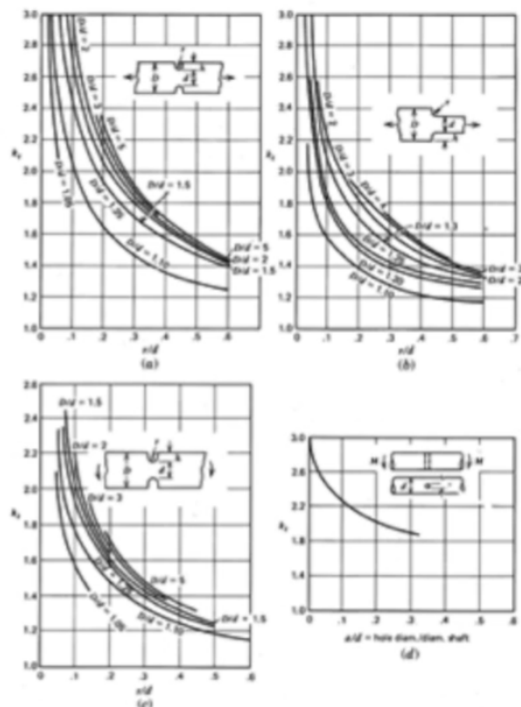


$$\frac{\sigma_{\max}}{\sigma_a} = 1 + \frac{2a}{b}$$

$$\sigma_{\max} = \sigma_a \left( 1 + 2 \sqrt{\frac{a}{\rho}} \right)$$

## Factors

Plastic deformation  
Engineering factors



# Stress concentration

Infinite stress!

$$\sigma_{\max} = \sigma_a \left( 1 + 2 \sqrt{\frac{a}{\rho}} \right)$$

## Crack:

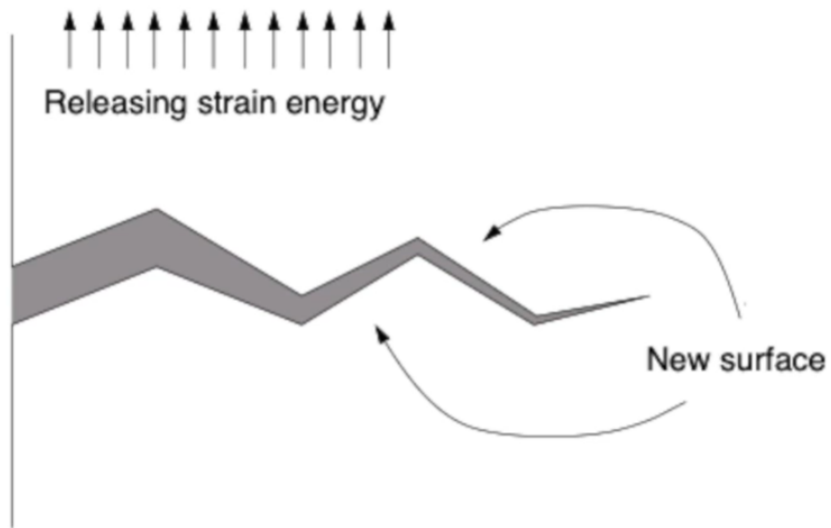
Elliptic flaw, for which

- tip radius is 0 and which thus
- causes infinite stress concentration



How materials  
endure *infinite*  
stress?

# Thermodynamic view



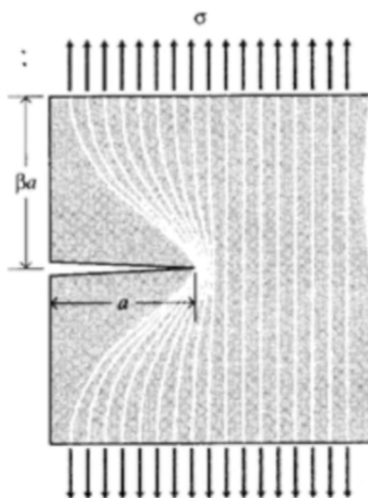
## Material strain energy

$$U^* = \frac{1}{V} \int f \, dx = \int \frac{f}{A} \frac{dx}{L} = \int \sigma \, d\varepsilon$$

## Unit volume

$$U^* = \frac{\sigma \varepsilon}{2} = \frac{\sigma^2}{2E}$$

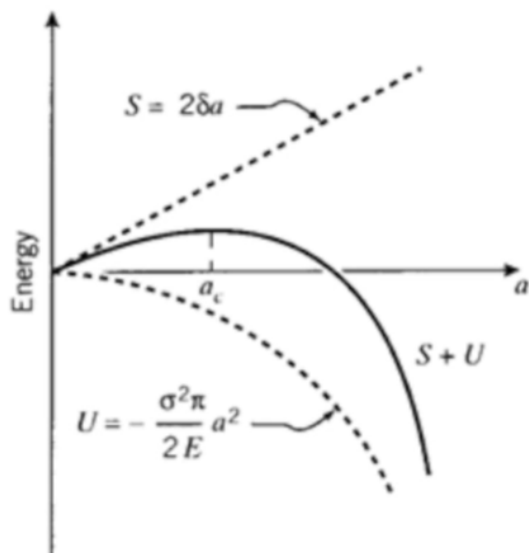
# Releasing strain energy



$$U = -\frac{\sigma^2}{2E} \cdot \pi a^2$$

Needed surface energy

$$S = 2\gamma a$$



## Fracture stress

$$-\frac{d\Pi}{dA} = \frac{dW}{dA} \Rightarrow \frac{\sigma^2}{E} \pi a = 2\gamma \Rightarrow \sigma_f = \sqrt{\frac{2E\gamma}{\pi a}}$$

## Griffith (1920)

Released energy is greater than required surface energy

Fracture stress depends on crack size

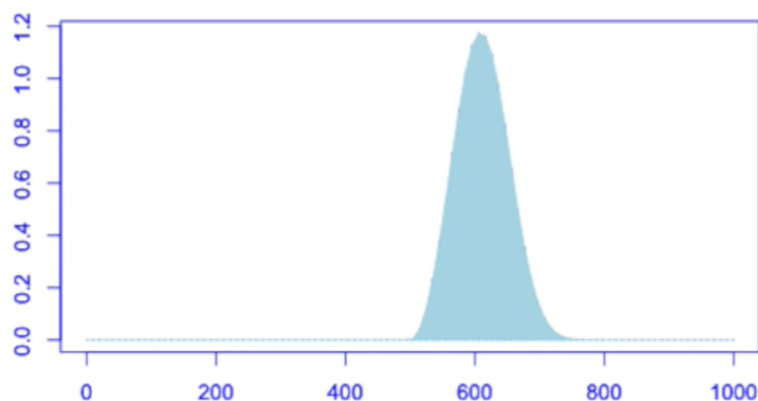
$$-\frac{d\Pi}{dA} = \frac{dW}{dA}$$

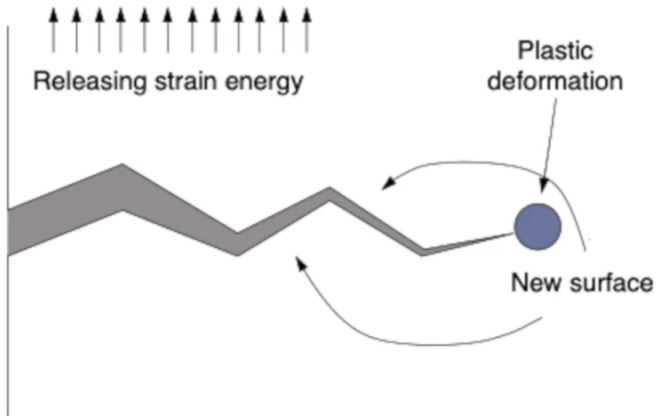
For brittle materials

$$\sigma_f = \sqrt{\frac{2E\gamma_s}{\pi a}}$$

## Ceramics: Strength below theoretical

... because the initial crack can start fracture which breaks atomic bonds one after another





## Irwin (1948)

**Plastic deformation spends energy**

**Energy release rate  $G$**

- Rate = /crack growth increment

$$\sigma_f = \sqrt{\frac{2E(\gamma_s + \gamma_p)}{\pi a}}$$

**Crack in a large plate:**

$$G = -\frac{d\Pi}{dA} \quad G = \frac{\pi\sigma^2 a}{E}$$

$$G_c = \frac{dW}{dA} = 2w_f$$

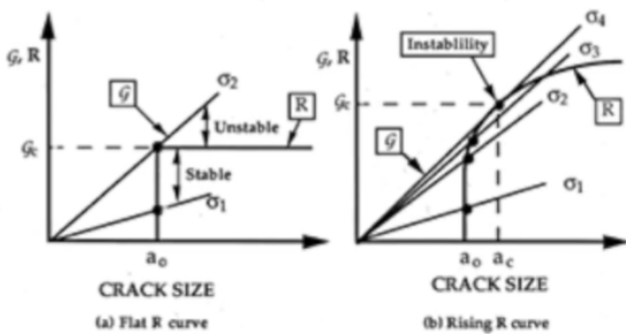
## R-curve (tearing curve)

**Crack grows when  $G > G_c$**

**Growth can be stable or unstable**

- Depends on crack growth effect to  $G_c$
- Unstable when

$$\frac{dG}{da} > \frac{dR}{da}$$



# Problems

Resolving G-level is laborious

How does the crack know the energy to be released?

## Crack stress concentration

Westergard (1939):

$$\sigma_y = \frac{p}{\sqrt{1 - \frac{a^2}{x^2}}}$$

$$2\eta = \frac{4(1-\mu^2)p}{E} \sqrt{a^2 - x^2}$$

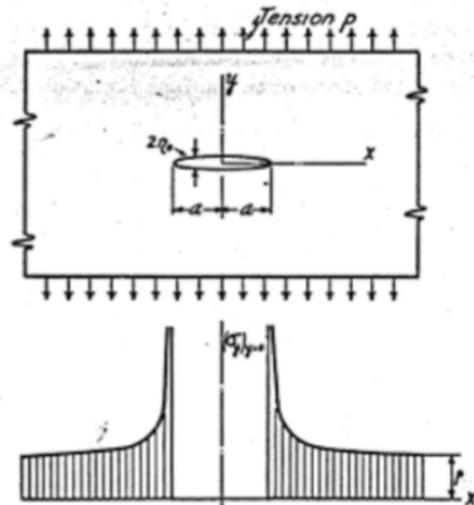


FIG. 4 INTERNAL CRACK

# Crack tip stress and K

Irwin (1957):

- Crack tip stress state can be resolved, when stress intensity factor (SIF) is known:

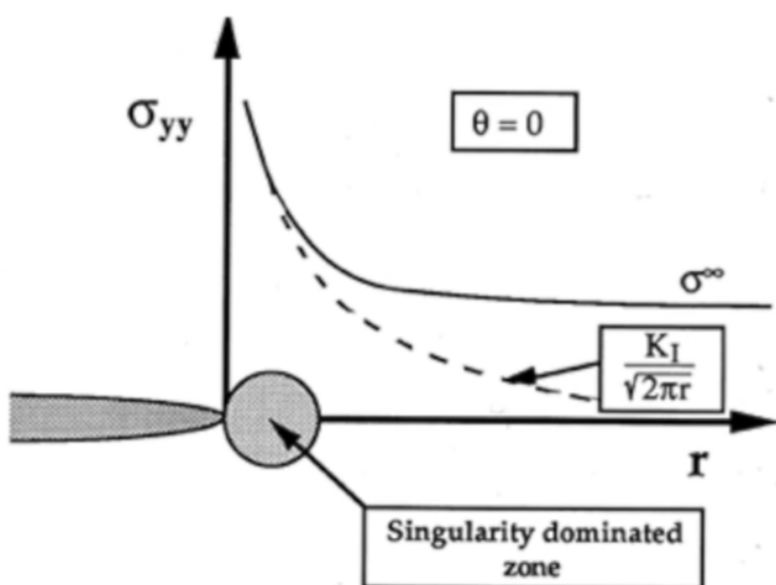
$$SIF = \sqrt{\frac{EG}{\pi}} = K$$

$$\sigma_{ij} = \frac{K}{\sqrt{2\pi}} f_{ij}(\theta) + \text{muista termejä}$$

K depends on the load situation and geometry

=> group of universal K-solutions

## Dominance zones

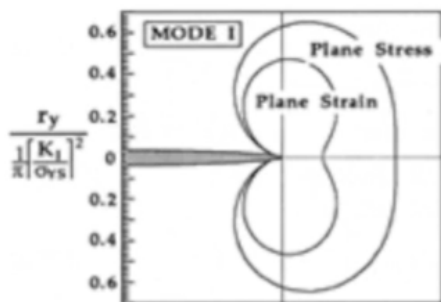
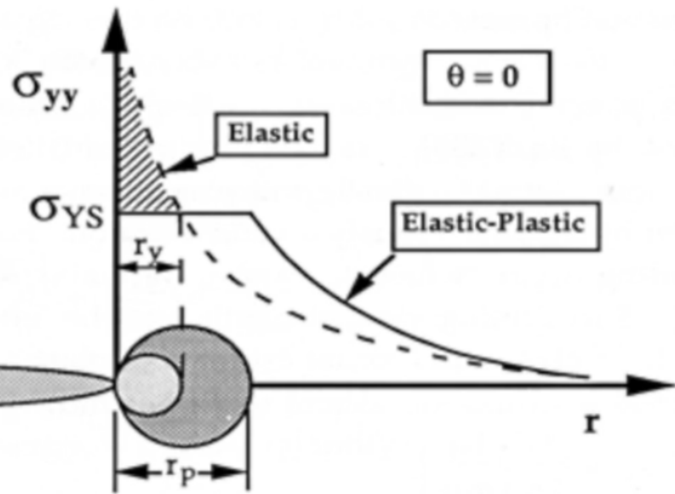


Plain strain

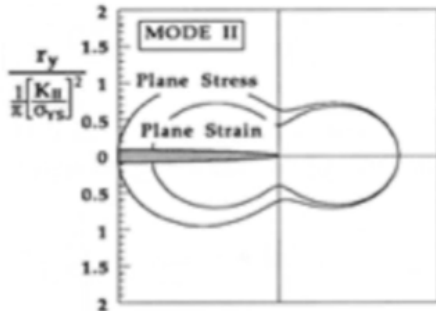
$$r_y = \frac{1}{6\pi} \left( \frac{K_I}{\sigma_{YS}} \right)^2$$

Plain stress

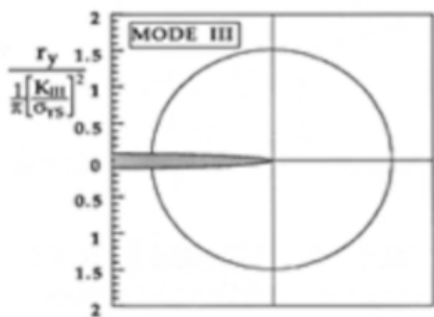
$$r_y = \frac{1}{2\pi} \left( \frac{K_I}{\sigma_{YS}} \right)^2$$



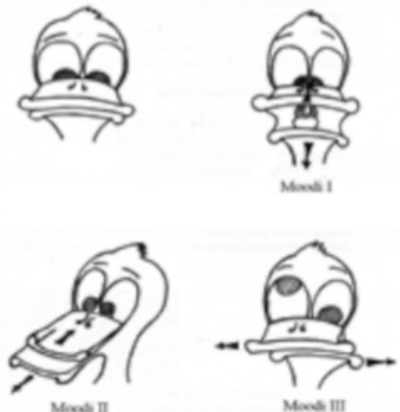
(a) Mode I



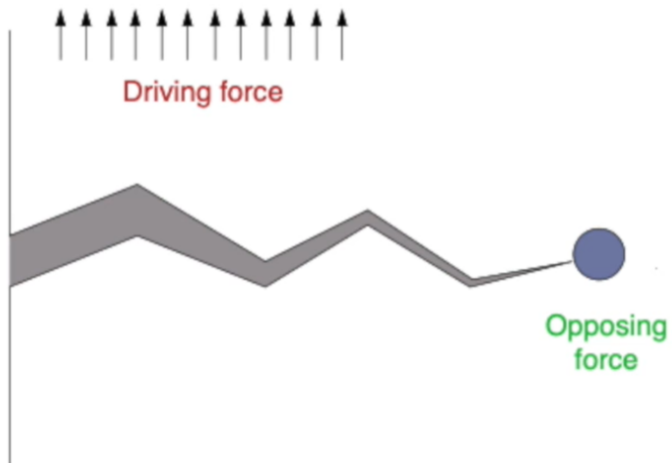
(b) Mode II



(c) Mode III



# Material susceptibility

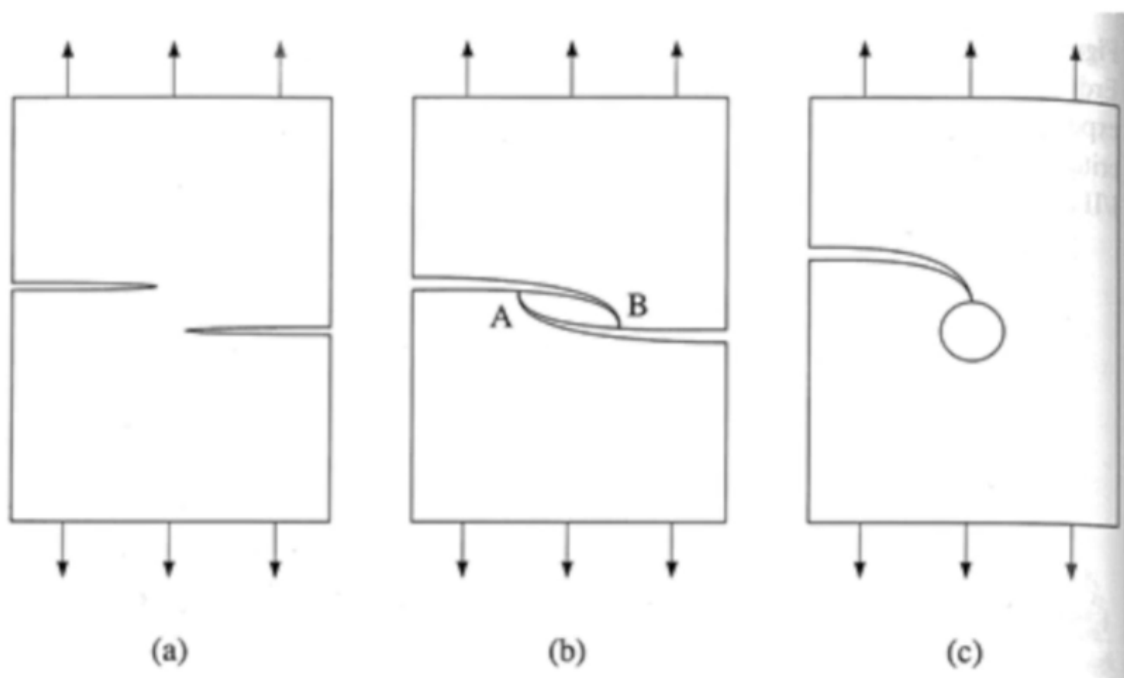


$K_{IC}$

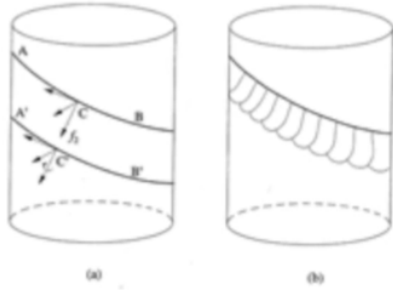
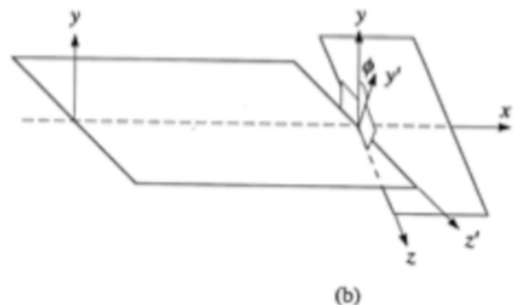
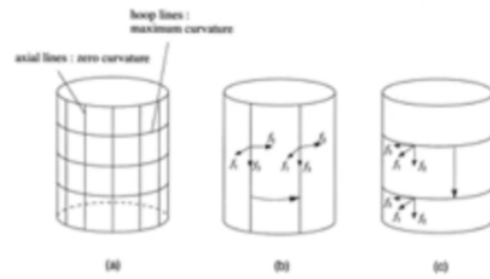
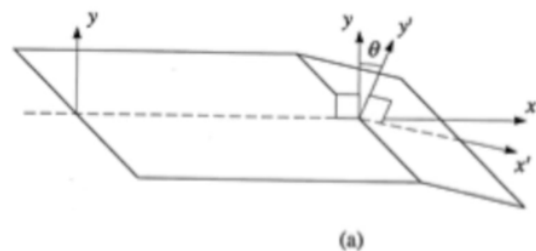
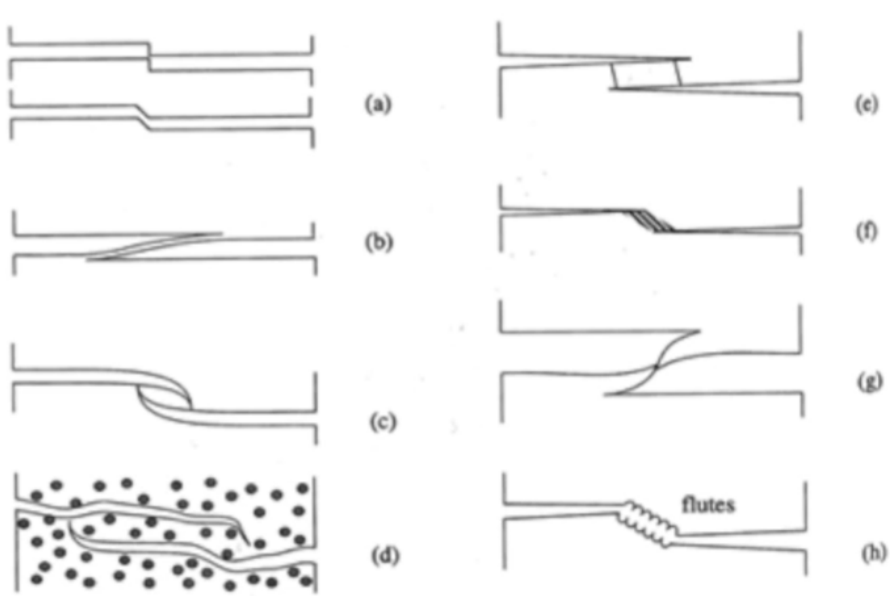
**Kritical value of K, which starts unstable fracture**

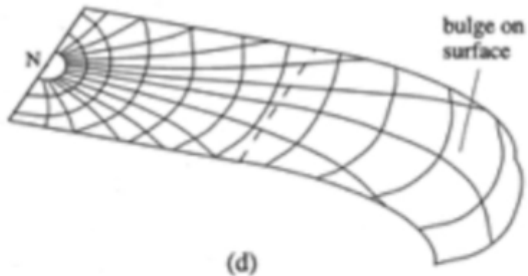
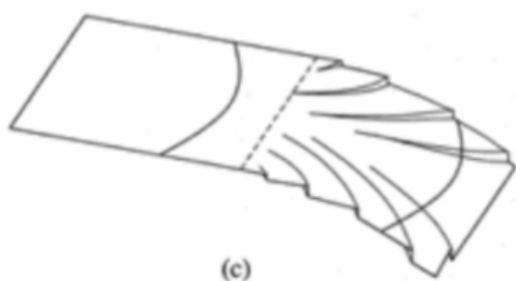
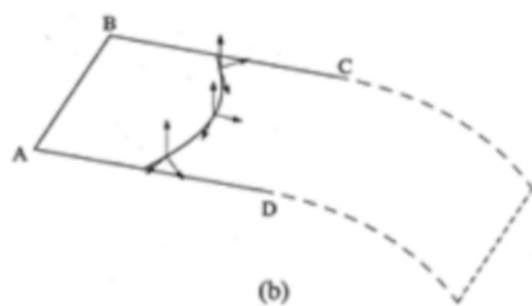
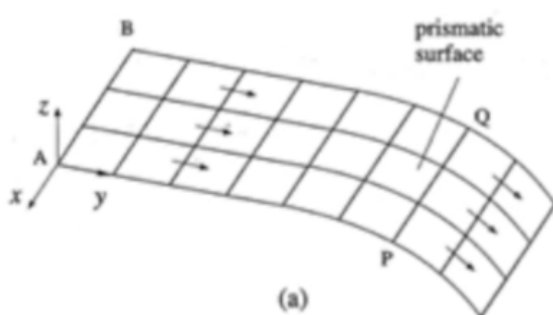
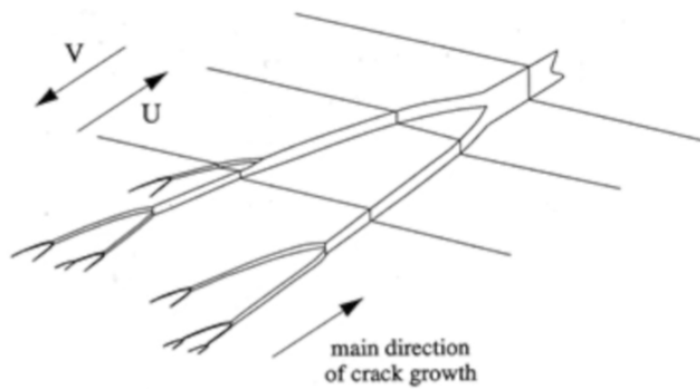
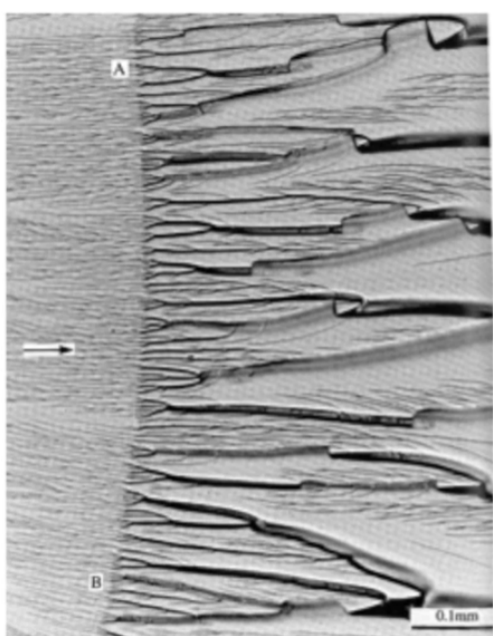
**Lowest measurable value**

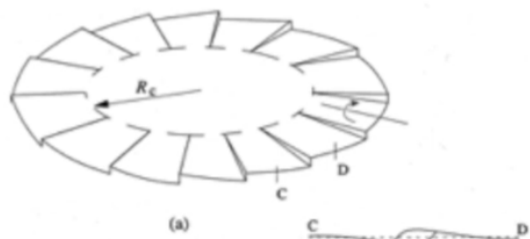
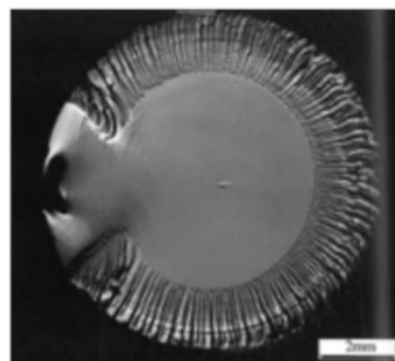
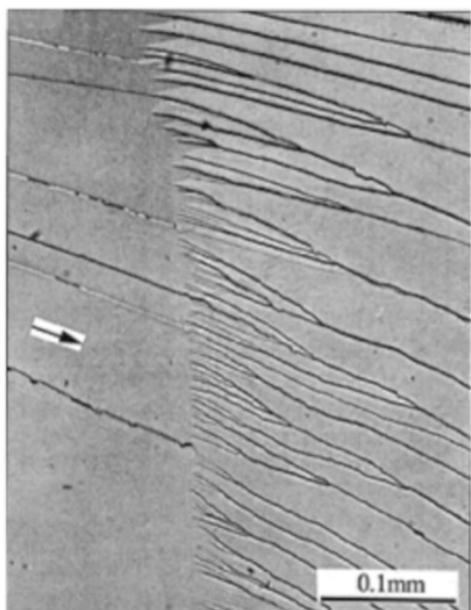
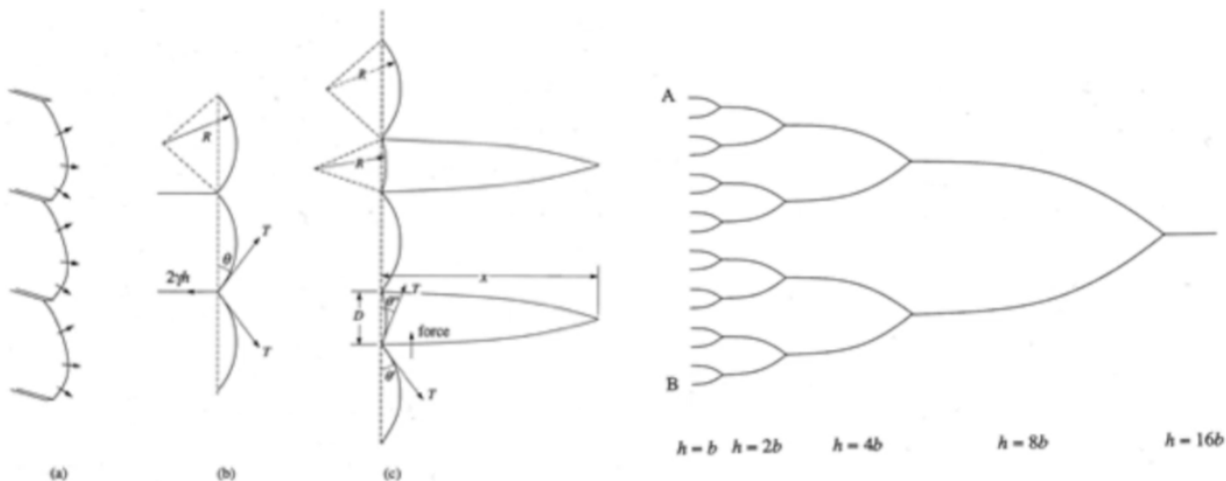
**Traditionally measured by loading cracked test piece**



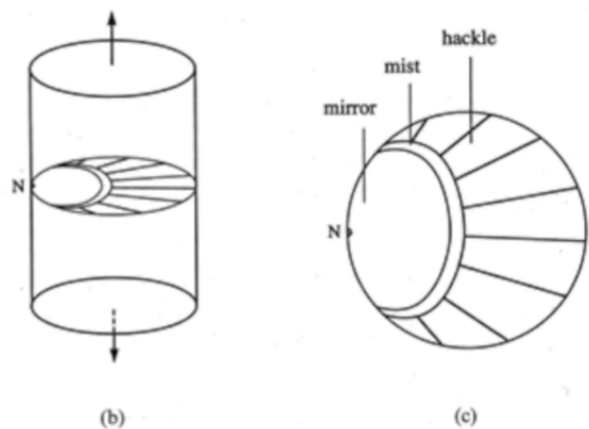
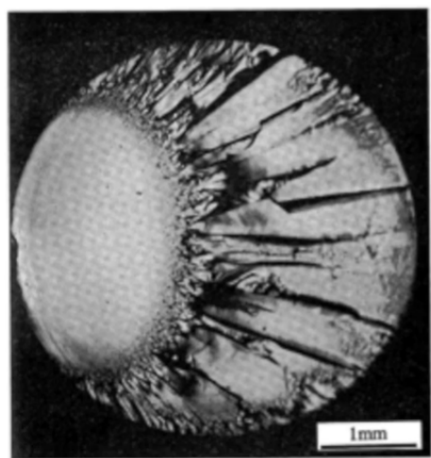
**Figure 4.33** Micro-mechanisms of deformation and fracture at overlapping cracks along river line steps: (a) simple cleavage, (b) delamination-type fracture characteristic of layer structures, (c) crack tilting in amorphous glasses, (d) crack tilting in multi-phase materials, (e) double cleavage, (f) simple shear failure, (g) ductile necking, (h) ductile flute formation.



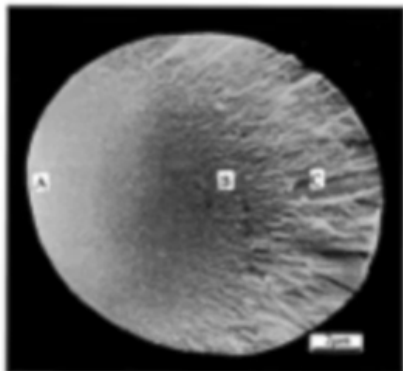




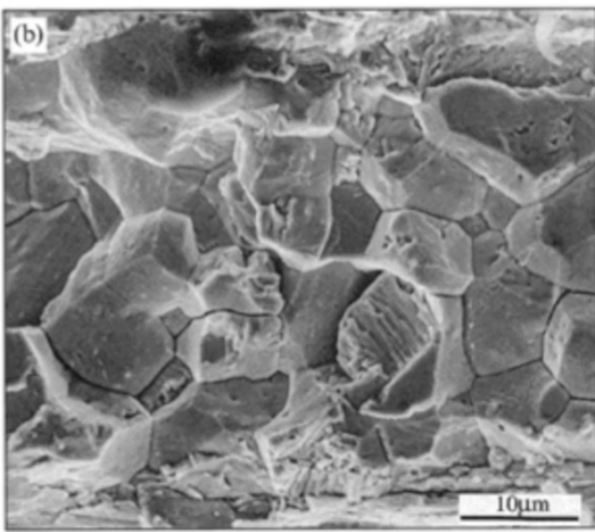
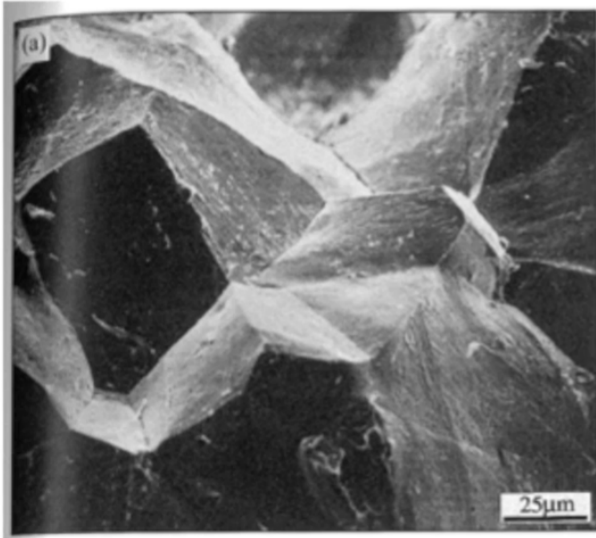
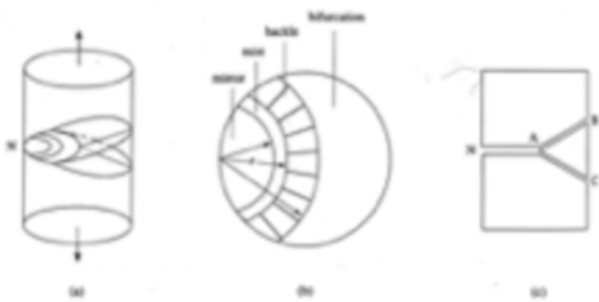
**Figure 5.1** Mirror, mist and hackle regions on fracture surface of a 5 mm diameter soda-lime-silica glass rod tested in uniaxial tension. Fracture nucleated at a small defect at N on surface of rod. (a) Light microscope photograph of fracture surface showing an approximately semi-circular mirror region bounded by narrow band of mist that developed into hackle. (b) Geometry of tensile test showing position of fracture surface normal to tensile axis. (c) Arrangement of mirror, mist and hackle regions on fracture surface. From Johnson and Holloway, see footnote (5.1).



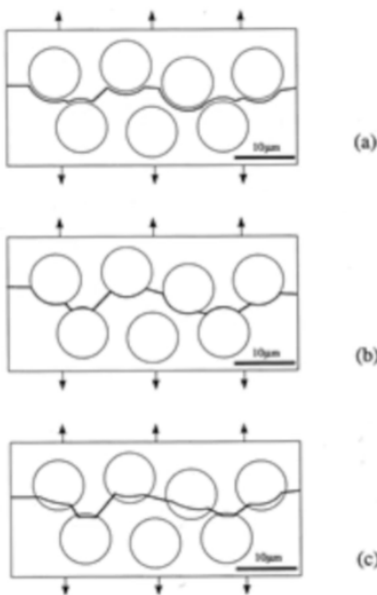
**Figure 5.2** SEM image of fracture surface of a 16  $\mu\text{m}$  diameter E-glass fibre. Surface was coated with a thin gold-palladium layer to prevent electrostatic charging in the microscope. Cross-section of fibre appears elliptical because fracture surface was tilted at an angle to the electron beam to obtain maximum contrast. Features of mirror (A), mist (B) and huckle (C) are almost identical to those in Fig. 5.1 but there is a large difference of scale.



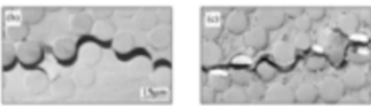
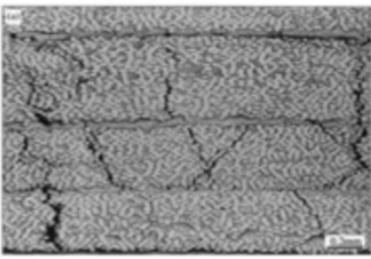
**Figure 5.3** Schematic of relationship between mirror, mist, huckle and macroscopic bifurcation in a rod specimen tested in uniaxial tension, for a crack nucleated at N on surface of rod: (a) geometry of test specimen and bifurcated cracks, (b) fracture surface appearance, (c) section through centre of fractured specimen parallel to tensile axis.



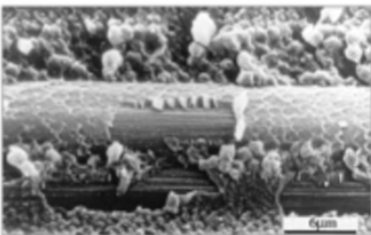
**Figure 7.6** Some possible fracture paths in unidirectional carbon fibre-polymer matrix resin tested in transverse tension.  
 (a) Fracture entirely through the matrix close to the fibres, associated with strongly bonded fibre-matrix interfaces.  
 (b) Cracks at weak fibre-matrix interfaces joined by matrix cracks.  
 (c) Fracture within fibre and through matrix.



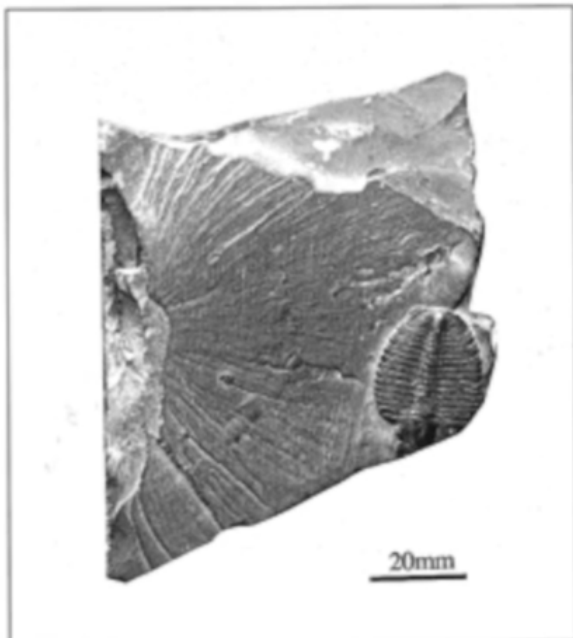
**Figure 7.7** Polished sections, viewed by light microscopy, illustrating transverse crack paths in glass fibre-cross-linked resin composites. (a) Multiple transverse cracks in a 2.5° angle-ply laminate based on glass resin, with relatively weak fibre-matrix interfaces. (b) Higher-magnification view of a similar material showing crack growth round fibres and through matrix. From M. L. C. Jones and D. Hull, Microscopy of failure mechanisms in composite materials, *J. Mat. Sci.*, 1979, 14, 765-774, 813. As for (a) with a strong fibre-matrix bond, vinyl ester matrix, showing cracks growing partly through fibres. From A. Spigoni, Matrix and Interface Effects on Macro-Cracking in Polymer Composites, PhD Thesis, 1997, University of Technology, Linköpings.



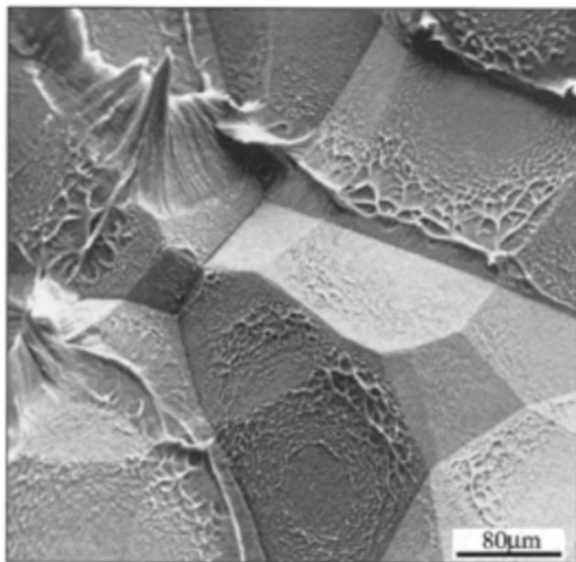
**Figure 7.8** SEM image of fracture surface of unidirectional carbon fibre-polymer matrix composite tested in transverse tension. Interface fracture has occurred partly at carbon fibre surface and partly at interface between epoxy resin particles and polypropylene. From Lowe, see Fig. 4.29.



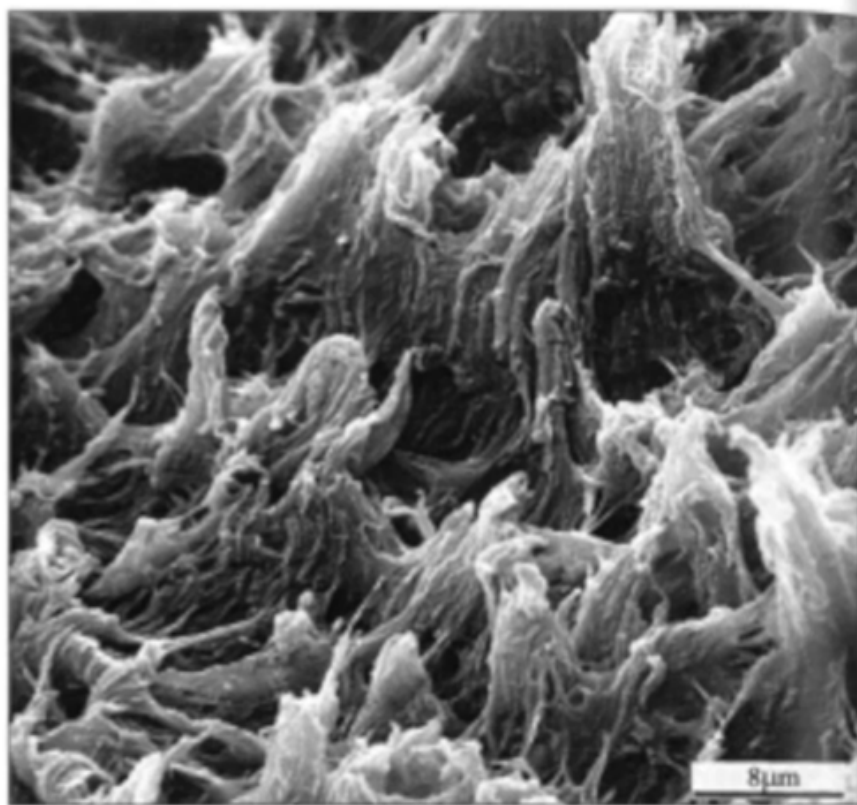
**Figure 7.17** Photograph of a trilobite fossil revealed by splitting a shale rock parallel to bedding plane. Crack path followed interface between fossil (hard calcite shell) and shale. Fracture surface of shale shows river lines that indicate a slight 'twisting' of crack during splitting and crack growing from left to right.



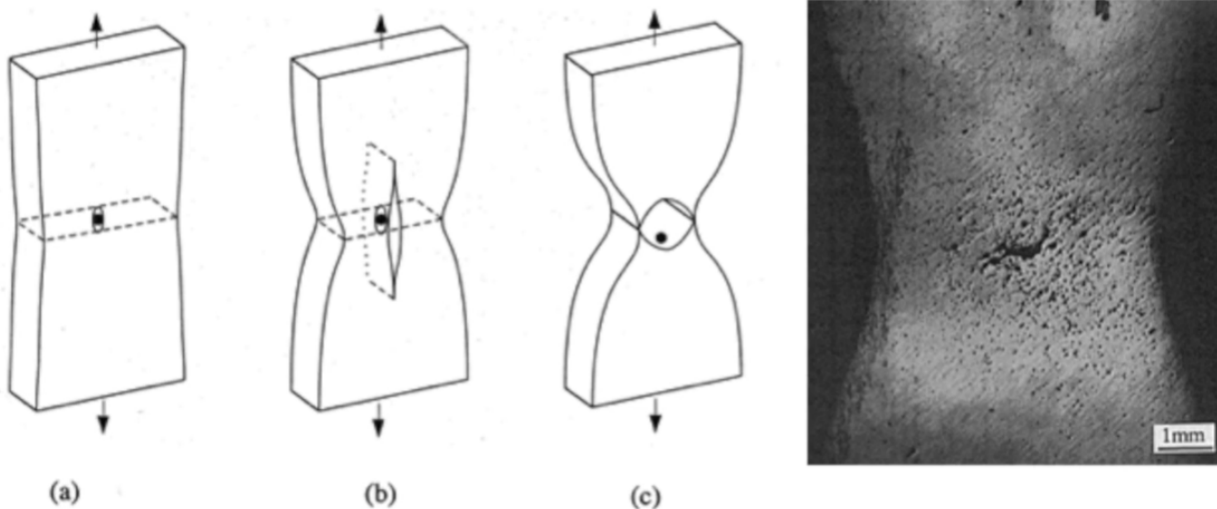
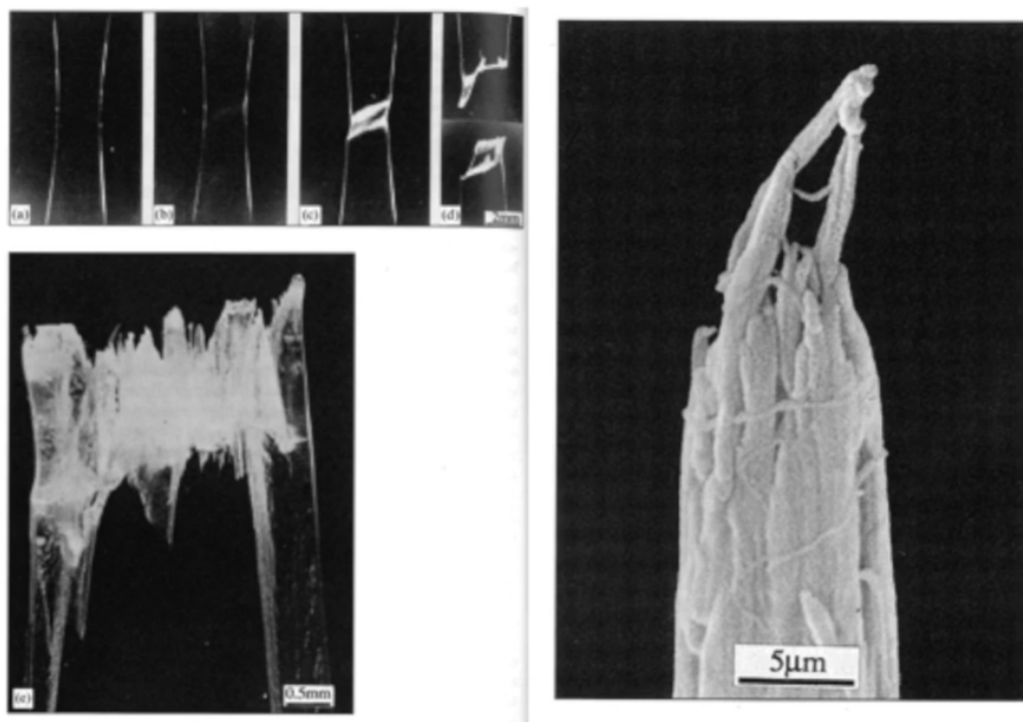
**Figure 7.19** SEM image of inter-spherulitic boundaries in a relatively low molecular weight polypropylene fractured in tension at room temperature. From K. Friedrich, Strength and fracture of crystalline isotactic polypropylene and the effect of molecular and morphological parameters, *Prog Colloid and Polymer Sci.*, 1979, **66**, 299–309.

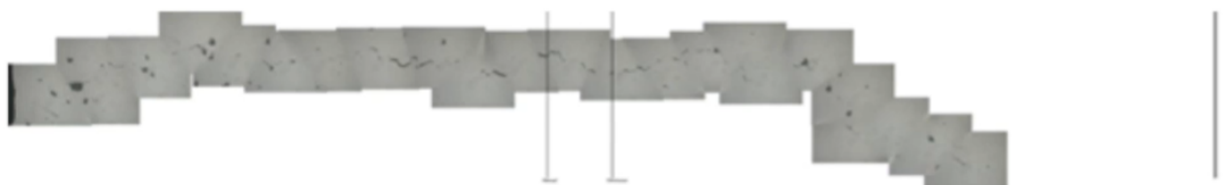
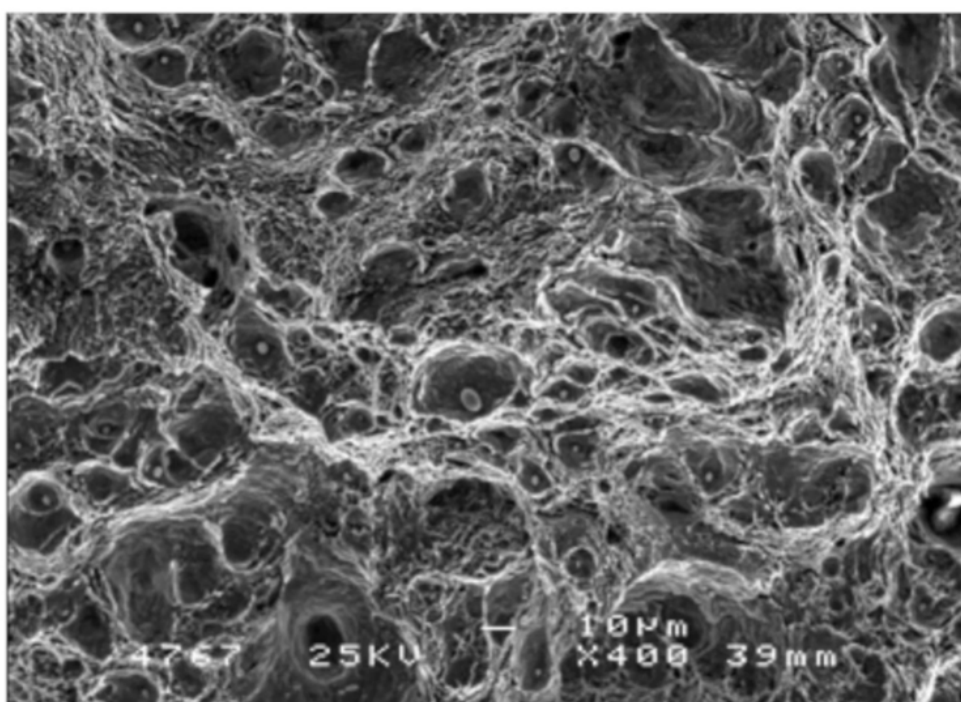


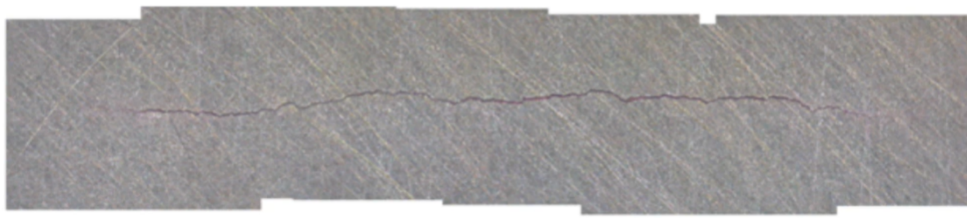
**Figure 8.1** SEM image of fracture surface of injection moulded semi-crystalline copolymer (TPX) based on poly(4-methylpentene-1). Specimen was fractured in uniaxial tension at 293 K normal to injection moulding direction. Image is from region of crack nucleation, marked by A in Fig. 8.2. The surface was coated with gold-palladium to minimise electro-static charging. Some local charging occurred at tips of fibrillated regions. Note: no other technique reveals the detail evident in this photograph. From T. W. Owen and D. Hull, Mechanical properties of injection moulded semi-crystalline plastics, *Plastics and Polymers*, 1974, **42**, 19–26.



**Figure 8.12** Example of local necking and fracture of a polystyrene specimen in which the molecules had been partly oriented in the tensile direction by hot drawing: (a) specimen before test, (b) initial stages of neck formation, (c) development of cold drawing, (d) local fracture in cold drawn region, (e) detail of fracture surface of a similar specimen showing extensive fibrillation. From L. Hoare, *Deformation and Fracture of Oriented Polystyrene*, PhD Thesis, 1975, University of Liverpool.





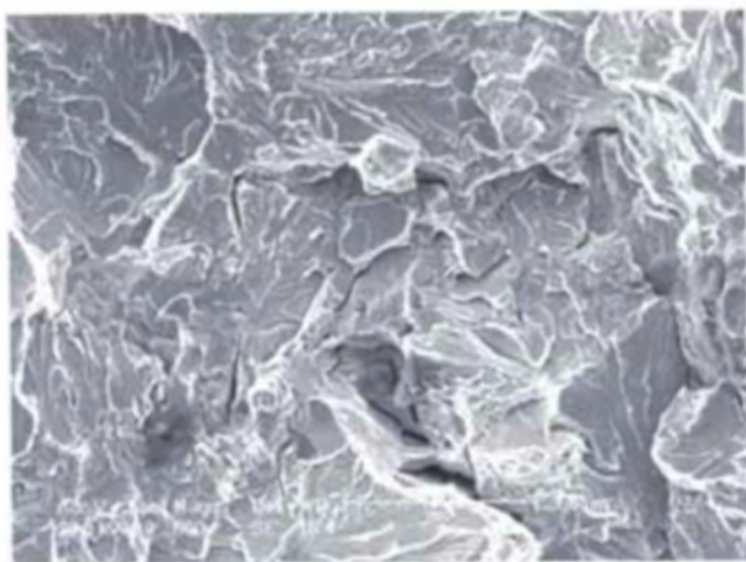


1 mm



1 mm

237AGB396



Kuva 9. SEM-kuva primäärimurtuman murtopinnasta.